THE IMPACT OF FATIGUE ON PREMOTOR BRAIN ACTIVITY

Juha Leukkunen

Masters' thesis in Biomechanics
Biology of physical activity
Jyväskylä University
Spring 2021
Supervisors: Janne Avela, Jan Wikgren & Simon Walker

TIIVISTELMÄ

Leukkunen, J. 2020. The impact of fatigue on premotor brain activity. Jyväskylän yliopisto, Biomekaniikan pro gradu -tutkielma, 75 s.

Fyysisessä väsymyksessä lihasten voimantuottokyky heikkenee. Esimotorinen aivojen aktivaatio on yhdistetty tiedostamattomiin liikkeen valmisteluun ja aloitukseen liittyviin toimintoihin. Valmiuspotentiaali on liikettä 1.5 sekuntia edeltävä negatiivinen jännitesiirtymä, jonka voimakkuus kuvaa kortikaalisen aktivaation suuruutta. Viimeaikaiset tutkimukset ovat osoittaneet ristiriitaisia tuloksia liittyen valmiuspotentiaalin muunteluun väsymyksessä. Osassa tutkimuksia valmiuspotentiaalin on osoitettu lisääntyvän ja osassa vähentyvän. Valmiuspotentiaalin on ehdotettu koostuvan sekä positiivisista että negatiivisista siirtymistä, ja että sen dynamiikka noudattaisi stokastista aaltoilevaa aktiivisuutta päätöksentekokynnyksen alapuolella. Positiivisten ja negatiivisten valmiuspotentiaalien voimakkuuden muuntelua ja niiden yhteyttä kortikospinaaliseen herkkyyteen ei ole aiemmin tutkittu väsymyksessä.

10 koehenkilöä osallistui ristikkäisasetelma-tutkimukseen, joka koostui kontrolli- ja väsytyskuormituksista. Molemmissa kuormituksissa suoritettiin 60 isometrista plantaarifleksiota jaettuna 30 suorituksen blokkeihin 1 ja 2. Valmiuspotentiaali mitattiin itsealoitetuista lihassupistuksista, joita toistettiin noin 20 sekunnin välein. Väsytyssupistuksissa (30 + 30) voimaa tuotettiin ensimmäinen neljä sekuntia 50 % maksimaalisesta isometrisesta lihassupistuksen (MVC) vääntömomentista, josta siirryttiin suoraan kolmen sekunnin maksimaaliseen supistukseen. Kontrollisupistuksissa (30 + 30) voimaa tuotettiin seitsemän sekuntia 10 % MVC vääntömomentista. Blokkien 1 ja 2 välissä pidettiin viiden minuutin tauko. Ennen blokkia 1 (PRE), blokkien 1 ja 2 välissä (POST1) ja blokin 2 jälkeen (POST2) mitattiin: 1) tahdonalaista aktivaatiota kortikaalisella transkraniaalisella magneettistimulaatiolla (TMS) sekä ääreishermon tasavirtastimulaatiolla, 2) kortikaalisen stimuluksen jälkeistä vaimentuneen lihasaktiivisuuden kestoa ja 3) kuormittuneisuuden tunnetta. Kortikospinaalista herkkyyttä mitattiin TMS:llä indusoitujen motoristen herätevasteiden rekrytointikäyränä ainoastaan PRE ja POST2.

Väsytyksen aikana MVC vääntömomentti laski väleillä PRE 291 ± 41 Nm ja POST1 211 ± 37 Nm ($p \leq 0.01$) sekä PRE ja POST2 200 ± 36 Nm ($p \leq 0.01$). Positiivisia valmiuspotentiaaleja (positiivisten ja negatiivisen valmiuspotentiaalien erotus) oli enemmän väsytyksessä (Block1 5.0 ± 12.9 ja Block2 2.0 ± 6.2) ja negatiivisia enemmän kontrollissa (Block1 -5.5 ± 6.2, $p \leq 0.05$ ja Block2 -6.0 ± 3.8, $p \leq 0.01$). Valmiuspotentiaalin voimakkuus lisääntyi 1.5 sekuntia ennen soleus-lihaksen lihasaktiivisuuden alkua. Väsytyksessä negatiivinen valmiuspotentiaali muuttui negatiivisemmaksi ja positiivinen positiivisemmaksi siirryttäessä kohti lihasaktiivisuuden alkua. Väsytyksessä positiivisen valmiuspotentiaalin myöhäisen komponentin RP2 pieneneminen blokkien 1 ja 2 välillä korreloi negatiivisesti ($r=-0.97$, $p=0.0063$, $n=5$) vääntömomentin vähenemisen kanssa välillä PRE ja POST2.

Tahdonalaisen aktivaation taso kortikaalisella stimulaatiolla laski väsytyksen aikana välillä PRE 91 ± 5 % ja POST2 80 ± 14 % ($p \leq 0.05$), ja ääreishermon stimulaatiolla väleillä PRE 99 ± 2 % ja POST1 89 ± 5 % ($p \leq 0.01$) sekä PRE ja POST2 93 ± 5 % ($p \leq 0.01$). Vaimentunut lihasaktiivisuuden jakso kortikaalisen stimuluksen jälkeen lyheni väsytyksen aikana väleillä PRE 0.144 ± 0.011 s ja POST1 0.132 ± 0.012 s ($p \leq 0.05$) sekä PRE ja POST2 0.134 ± 0.011 s ($p \leq 0.05$). Kuormittuneisuuden tunne lisääntyi väsytyksen aikana väleillä PRE 1.2 ± 2.3 ja POST1 6.7 ± 2.2 ($p \leq 0.01$) sekä PRE ja POST2 8.4 ± 2.0 ($p \leq 0.001$). Rekrytointikäyrän voimakkuus vääntömomentin tasolla 20%MVC vääntömomentista lisääntyi yhtenevästi kontrollin ja väsytyksen aikana, mutta ei merkitsevästi.

Tutkimuksen mukaan väsymystä aiheuttava intervallityyppinen maksimaalinen isometrinen plantaarifleksio-kuormitus muuntelee positiivisten ja negatiivisten valmiuspotentiaalien osuuksia yhdessä maksimaalisen vääntömomentin laskun kanssa, mikä indikoi ei-optimaalista vähentyneen herkkyyden tilaa motorisen aivokuoren hermosoluverkoissa liikkeen aloituksen aikana suurimmassa osassa lihassupistuksia.

Asiasanat: kortikospinaalinen herkkyys, EEG, väsymys, maksimaalinen tahdonalainen lihassupistus, motorinen ohjaus, ääreishermon sähköstimulaatio, esimotorinen aktivaatio, valmiuspotentiaali, rekrytointikäyrä, tahdonalainen aktivaatio

ABSTRACT

Leukkunen, J. 2020. The impact of fatigue on premotor brain activity. University of Jyväskylä, Master's thesis in Biomechanics, 75 pp.

Ability to generate force decreases during performance fatigue. Premotor activity has been connected to unconscious processes related to movement preparation and ignition. Readiness potential (RP) is a cortical voltage drift preceding movement onset by 1.5-s and its negative amplitude is a marker of neural activity. Recent studies have shown conflicting results about RP amplitude both increasing and decreasing during fatigue. It has been suggested that RP consists of both positive and negative shifts, is based on a stochastic fluctuating activity under decision threshold, and is probabilistic in nature. Slope-dependent RP amplitude modulation during fatigue and how it is linked to corticospinal excitability (CSE) has not been previously studied.

10 volunteers participated in a crossover study fatiguing and control protocol of 60 isometric plantar flexions divided into blocks 1 and 2 of 30 contractions each. Contractions were self-started every ~20-s and RP was measured. Fatiguing contractions (30 + 30) started with 4-s at 50%MVC and ended in 3-s maximal contraction, while control contraction lasted 7-s at 10%MVC. There was a 5-min break between blocks. Cortical and peripheral voluntary activation level (CVAL and PVAL, respectively), cortical silent period (SP), and rating of perceived exertion (RPE) was measured before Block1 (PRE) and between and after Block1 (POST1) and 2 (POST2). Recruitment curve was measured with transcranial magnetic stimulation (TMS) only at PRE and POST2.

The fatiguing protocol resulted in a significant decrease in MVC torque from PRE (291±41Nm), to POST1 (211±37Nm) and POST2 (200±36Nm). There was a significantly larger occurrence of RPs with positive slope (measured as a difference in number of positively and negatively categorized RPs) during fatiguing contractions (Block1 5.0±12.9 and Block2 2.0±6.2) and significantly larger amount of negative RPs during control contractions (Block1 -5.5±6.2 and Block2 -6.0±3.8). RP amplitude showed a significant effect of time starting 1.5-s before electromyographic (EMG) activity of the soleus muscle (SOL). Negative RPs amplitude got more negative during control and positive RPs got more positive during fatigue closer to EMG onset. During fatigue a significant negative correlation ($r=-0.97$, $p=0.0063$, $n=5$) was found between decrease in positive RP2 amplitude from Block1 to Block2 and decrease in torque from PRE to POST2.

During fatigue CVAL (PRE 91±5% to POST2 80±14%), PVAL (PRE 99±2% to POST1 89±5% and PRE to POST2 93±5%), cortical SP (PRE 0.144±0.011-s to POST1 0.132±0.012-s and PRE to POST2 0.134±0.011-s) were significantly reduced while RPE was significantly increased (PRE 1.2±2.3 to POST1 6.7±2.2 and PRE to POST2 8.4±2.0). Recruitment curve during 20%MVC showed a non-significant increasing trend in both conditions.

In conclusion, fatiguing intermittent maximal isometric plantar flexion exercise modulated the distribution of slope-dependent RPs concomitant with a decrease in MVC torque, which indicates suboptimal decreased excitatory state of M1 cortex neural circuits during movement ignition in the higher proportion of the contractions.

Key words: Bereitschaftspotential, cortical silent period, corticospinal excitability, EEG, fatigue, maximal voluntary contraction, motor control, peripheral nerve stimulation, premotor activity, readiness potential, recruitment curve, voluntary activation level

ABBREVIATIONS

AMT	Active motor threshold
AURC	The total area under the recruitment curve
BL	Baseline
CNS	Central nervous system
CSE	Corticospinal excitability
DS	Direct current stimulation
EEG	Electroencephalography
EMG	Electromyography
M1	Primary motor cortex
MEP	Motor evoked potential
Mmax	Maximum compound muscle action potential
MNE	MNE-Python open-source software package
MSO	Maximal stimulator output
MTAT	Motor threshold assessment tool
MU	Motor unit
NS’	Negative slope
RP	Readiness potential
RPE	Rating of perceived exertion
SD	Standard deviation
SIT	Superimposed twitch
SOL	Soleus
SP	Silent period
TA	Tibialis anterior
TMS	Transcranial magnetic stimulation
VAS	Visual analog scale

TABLE OF CONTENTS

1. INTRODUCTION

Physical and/or exercise performance is defined as an ability to produce movement or resist external forces, and it is a prerequisite in many sports requiring muscle contractions. Movement is generated when muscles produces necessary torque over movement related joints to overcome limbs gravity and/or momentum and possible external force.

Physical fatigue synonym to muscle fatigue has multiple definitions (Hunter 2018): increased effort to maintain constant power or force output (Enoka & Stuart 1985; Hunter 2018), exercise-induced acute reduction in motor performance (Hunter 2018), and reduced maximal voluntary force or power (Bigland–Ritchie 1984; Gandevia 2001; Hunter 2018). It is observed when subject fails to complete task in a specific time constraint or is unable to produce necessary torque over joints (Enoka & Duchateau 2016).

It has been shown during brief maximal voluntary contractions (MVC) in a prolonged isometric submaximal fatiguing elbow flexor contraction and during intermittent maximal plantar flexions (Kawakami et al. 2000; Søgaard et al. 2006) that torque production is not limited by the contractility of the muscle, but by the excitatory voluntary motor drive from the central nervous system (CNS). Also energy depletion and increased acidification in the working muscles has shown to not limit performance in an incremental whole-body (Morales–Alamo et al. 2015) and plantar flexion exercise till exhaustion (Hogan et al. 1999).

At cortical level several different brain regions together constructs the descending motor command (Zagrean et al. 2013, 423). Fatigue-related reduced motor drive is thought arise from a subconscious protective mechanism "central governor" that preserves muscle from catastrophic contraction failure (Noakes et al. 2005). In perception of exertion both physiological aspects are integrated with psychological factors (de Morree et al. 2012; McCormick et al. 2015). Afferent feedback from the contracting muscle modulates motor drive at many levels of the corticospinal motor pathway in periphery, spinal cord, and cortex. In sensorimotor transformation, selection of motor actions is guided by perception that gets sensory information as an input (Zagrean et al. 2013, 423). During fatigue information from afferents and motor command is send to primary motor cortex (M1) and cerebellum through direct and indirect negative feedback loops (Hureau et al. 2018; McMorris et al. 2018). Modulation prevents mo-

tor units (MU) from hyperactivation and premature fatigue, which could expose to transmission failure and suboptimal MU activation pattern. Also sarcolemma can have a protective role by reducing its conductivity especially in fast twitch muscle fibers during fatigue (Piitulainen 2010). Afferent feedback can be inhibitory or facilitatory depending on the phase of the task and fatigue, and its strength is proportional to the recruited muscle mass (Rossman et al. 2012). The amount of negative feedback leading to task failure is defined as the sensory tolerance limit (Gandevia 2001; Hureau et al. 2018).

Sensorimotoric functions and processes can be inspected centrally as changes in CNS, which consists of brains, spinal tract and motor nerves, and peripherally, distal from the neuromuscular junction. Cortical mechanisms of fatigue are less examined than spinal and peripheral ones. At cortical level studies have focused on the state of primary motor cortex at specific time point relative to muscle contraction. Often used method has been transcranial magnetic stimulation (TMS) combined with peripheral electric nerve stimulation (DS) to measure corticospinal excitability (CSE) and voluntary activation level (VAL). Simultaneous measurement of several brain regions have used magnetic resonance imaging (MRI), functional near-infrared spectroscopy (fNIRS), electroencephaloraphy (EEG), magnetoencephalography (MEG) and positron emission tomography (PET).

During state of increased excitability (depolarization) the closer and more uniform the inner-membrane voltages of neurons become near their discharge thresholds, the smaller excitatory input is needed to discharge the neural circuit. Inhibition, the decrease in neuron inner-membrane voltage (repolarization) caused by influx of negative ions (i.e. chloride and bicarbonate) prevents overexcitation of neurons (Farrant & Nusser 2005). Target neuron can optimise temporal summation of input from other neurons (Spruston 2008) using direct and indirect self-inhibition. Both increased excitability and inhibition are measured at M1 cortex during voluntary contraction in fatigue (Gandevia 2001), which is explained by activation of distinct neural circuits and/or alternating responses of same circuits to different activation protocols.

Interesting phenomena relating to voluntary contraction is premotor brain activity and movement related cortical potentials, which are measured using EEG and MEG. Readiness potential (RP) also referenced as "Bereitschaftspotential" or movement-related potential is a direct

current drift starting 2 to 1.5-s before muscle activity and is evoked by self ignited voluntary or imagined contraction (Deecke et al. 1976; Jankelowitz & Colebatch 2002; Jo et al. 2013). RP is not so prone to artefacts from the activation of effector muscle, while still serving as an online measure. It acts as a precursor for the final motor command that is buffered in M1 cortex and released at the appropriate time downward to corticospinal pathway. Stronger RP has been connected to the increasing excitability of neural networks at M1 cortex (Deecke et al. 1976). RP originates from the activity of contralateral supplementary motor area, cingulate gurys and bilateral M1 cortex (Cui & Deecke 1999). Supplementary motor area, premotor cortex and M1 cortex receives information about the decision to continue current task from lateral prefrontal cortex, which integrates information from somatosensory cortex and subcortical structures related to control of behaviour and emotional responses. (McMorris et al. 2018.)

Currently the field of fatigue research lacks studies using online cortical measurements during voluntary contraction. Goal of this study was to measure neural mechanisms of fatigue during voluntary activation, when cortical and motoneuronal excitability increases (Hoffman et al. 2009; Gandevia 2001; Taylor & Gandevia 2008) to take into account activation specific nature of fatigue (Taube et al. 2015). Central fatigue measured as VAL was determined both cortically and peripherally to inspect changes in motor output generating ability of cortical neural circuits and motoneuron responsiveness (Todd et al. 2003). Understanding the determinants of acute fatigue helps to profile performance limiting factors and guide athlete preparation and training periodisation.

2. PREMOTOR BRAIN ACTIVITY

Information processing leading to action. Interaction with the environment requires understanding of the physical and mental context, and transforming information between sensory and motor systems (Cisek et al. 2010). Information is stored into spatiotemporal activity patterns of neural circuits and one circuit may share many functions. Discharge frequency of a neuron is probabilistic in nature, meaning fixed input results in varying responses. Behavioural or cognitive functions in the cerebral cortex are organized into multiple neural circuits. (Sanger 2003.) In sensorimotor transformation, sensory information is converted for perception to form a model, which is mirrored against subjects experience about the world to guide decision making between motor actions that are finally executed (Cisek et al. 2010). Premotor and primary motor areas co-operate with associative and sensory areas constantly predicting and updating the sensorimotor transformation (Zagrean et al. 2013, 423). During premotoric time, parallel processing of timing, decision to act, preparation of movement and initiation of movement are organized through sensorimotor loops between cortex, thalamus, basal ganglia, red nucleus in the midbrain and cerebellum (Houk et al. 1993; Rektor et al. 2001; Schmahmann & Pandya 1990).

2.1. Action selection

Motor command is a set of movement instructions generated in the premotor brain areas, from where it is delivered to M1 cortex as a movement model and sent via descending pathway through spine and motoneurons to contracting muscle fibers. In extent of M1 cortex other regions i.e. the brainstem, basal ganglia, cerebellum and spinal cord support motor output through direct and indirect pathways (Atasavun & Düger 2020; Rosenbaum 2010). A copy of the signal is also sent to cerebellum, to predict and compare actual sensory feedback, and to make fine adjustments. Motor actions goes through competition during action selection. Sensory information is integrated into action selection and competition is modulated from the subcortical and prefrontal areas (figure 1).

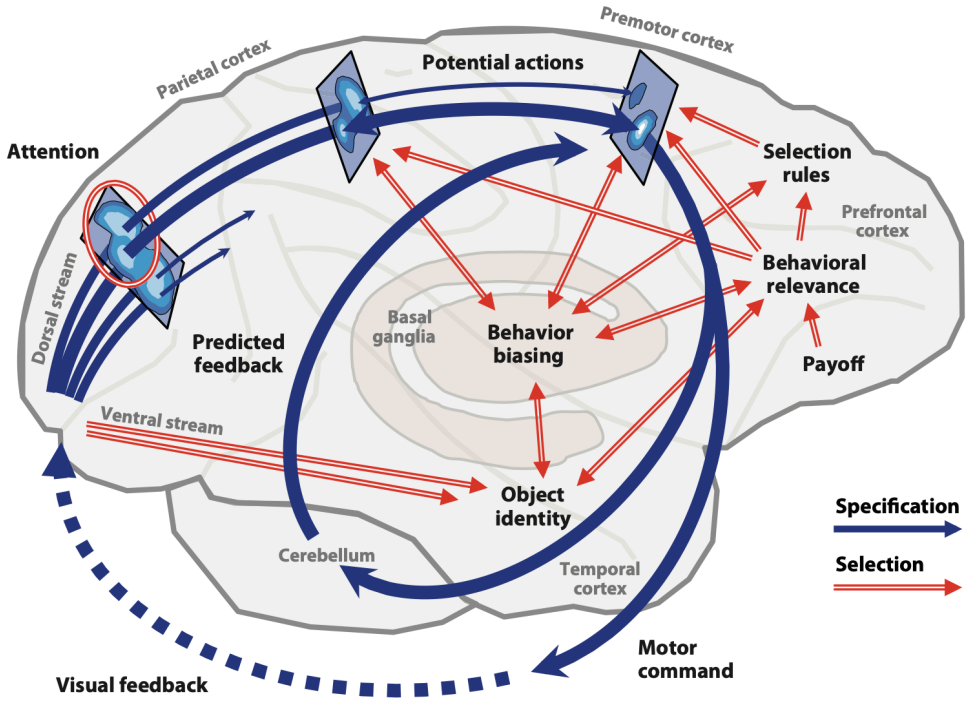

FIGURE 1. Illustration of different streams and circuits in the pipeline converting information from the environment into sensory coordinates and into action instructions. Brains are displayed anterior–posteriorly from right to left, respectively. Blue planes show activity maps of competing neuronal populations where population activity peaks at the lightest regions. Red line arrows correspond to the modulating input from areas that are responsible for action selection such as deeper structure basal ganglia and anterior prefrontal cortical areas. Pipeline ends from posterior sensory areas into centrally located primary motor cortex, which outputs a motor command into spinal cord. Cerebellum receives a copy (blue dotted line) of the motor command and a prediction of the sensory feedback. (from Cisek et al. 2010)

2.2. Temporal profile of premotor activity

During movement preparation there are electrophysiological changes in cortical parietofrontal areas. A slow negative shift begins 3-s before onset of electromyographic (EMG) activity in the superior parietal lobule in the somatosensory cortex. Simultaneously there is event-related desynchronization of rhythmic activity in the β-band (18–22Hz) in the contralateral and mid-line sensorimotor and posterior parietal areas. (Wheaton et al. 2005.) Phasic inhibition is used to generate and maintain rhythmic synchronous activity between neurons and brain regions (Spruston 2008). Event-related desynchronization is connected to neural circuits changing from idling state to be ready for transferring information (Wheaton et al. 2005). 2-s before

movement onset negative shift starts to spread bilaterally towards premotor areas (Wheaton et al. 2005), especially supplementary motor area (Ikeda et al. 1995), while event-related de-synchronization at β-band concentrates contralaterally and is maximized. Parietal areas are responsible of processing general task related information, whereas premotor areas are more specific adding precision in complex movements. Premotor areas are involved in movement ignition and memory-guided movements. (Wheaton et al. 2005.)

RP belongs to movement-related cortical potentials, which is a subclass of (Berchicci et al. 2013) event-related potentials, cortical time-locked responses to specific events and sensory stimuli (Blackwood & Muir 1990). RP is usually described as a weak ~10μV negative direct current drift preceding movement onset, calculated by taking average across multiple epochs (figure 2). When single epochs are inspected, there are both negative and positive shifts, and the proportion of negative shifts is slightly larger (Jo et al. 2013). RP reflects cortical spontaneous fluctuating synchronous post-synaptic activity related to initiation of movement (Deecke et al. 1976; Jo et al. 2013; Wheaton et al. 2005). The increase in neuronal activity is associated with increased RP amplitude, whereas attenuation represents decreasing activity (Deecke et al. 1976).

Early RP components are divided into readiness potential 1 (RP1) from 1.5 to 1.0-s before onset and readiness potential 2 (RP2) from 1.0 to 0.5-s before onset. Late RP has two subcomponents negative slope (NS') from 0.5 to 0-s before EMG/force onset and motor potential (MP), the peak amplitude from 0.5 to 0-s before onset (Spring et al. 2016). RP components are described as a time window mean or peak amplitudes or area under the curve (Shibasaki & Hallett 2006). Early RP increases with speed of the movement, while late RP increases in complex and isolated movements requiring more precision e.g. "monospike" recruitment of single motor unit. Other modulating factors are movement type, preparatory state, perceived effort, force, level of intention, movement selection and pace of movement repetition. (Kato & Tanji 1972; Shibasaki & Hallett 2006.)

Premotor activity ends in MP, that describes how many motor units are initially recruited and what is the initial frequency of α-motoneurons. MP amplitude is modulated by movement parameters and its strength is reflected with the initial slope of rectified EMG from 0.1 before to

0.5-s after force onset. (Johnston et al. 2001.) M1 cortex excitability starts to increase 100-ms before EMG onset during self-paced movements and corresponds with MP (Chen et al. 1998).

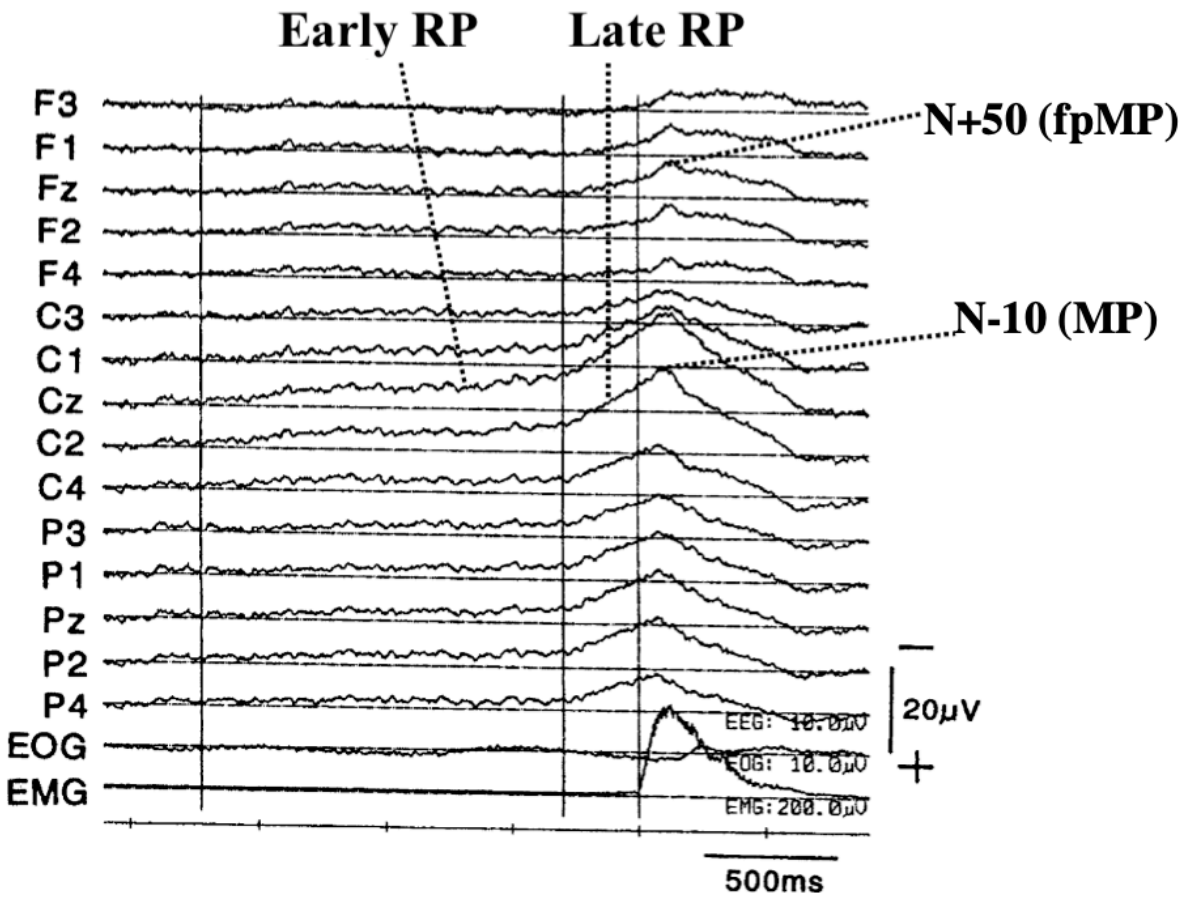

FIGURE 2. Bereitschaftspotential also known as readiness potential as a negative shift preceding onset of muscle activity (rightmost crossing vertical line) at several scalp electrodes (F=frontal, C=central, p=parietal, odd=left hemisphere, even=right hemisphere, z=midline) using linked ear electrodes as a reference. RP=readiness potential (RP), MP=motor potential, fpMP=frontal peak of motor potential, EMG=electromyography, EOG=electrooculography. (modified from Shibasaki & Hallett 2006.)

RP has been suggested to be a continuous stochastic process of spontaneous fluctuating activity under decision threshold, that could explain both negative and positive drifts during initiation of movement and irrespective to any external events (Schurger et al. 2012). Against this model Travers et al. (2020) showed that these RP like events measured outside of voluntary actions to be false positives.

RP integrates current, predicted and expected sensory feedback in supplementary motor area and M1 cortex (Haggard & Tsakiris 2009; Wen et al. 2018). Early RP activity from 1.5 to 0.5-s before EMG/force onset is connected to supplementary motor area and prefrontal areas, and later contralateral activity from 0.5 to 0-s before onset to premotor cortex, M1 cortex (Ikeda et al. 1995; Shibasaki & Hallett 2006) and pyramidal tract neurons (Shibata et al. 1997).

During movement preparation there are interactions between cortical and subcortical, and central and parietal areas. M1 cortex and association cortices receives facilitatory input th-rough loops from the ventral lateral nucleus of thalamus, which also receives input from cere-bellum. Similar cortical RP with a reversed polarity is shown in the ventral lateral nucleus of thalamus, subthalamic nucleus and basal ganglia (Paradiso et al. 2003; Paradiso et al. 2004; Rektor et al. 2001). Supplementary motor area and thalamus are also known to have premo-vement interaction via β rhythm (~20Hz) (Paradiso et al. 2004).

2.3. Premotor areas

Premotor cortex (figure 3) modulates the timing of the different phases of the motor task, synchrony and timing of proximal muscle activation and controls tasks involving precise posi-tioning of the effectors (Chouinard & Paus 2006; Davare et al. 2006). M1 cortex pyramidal neurons excitability is modulated via interneurons through cortico-cortical connections from premotor cortex and supplementary motor area (Arai et al. 2012; Bäumer et al. 2009; Münc-hau et al. 2002). Premotor cortex is activated in several circumstances not directly related to fatigue, but could have a role in modulating M1 cortex and especially early part of RP. These conditions include spatial, object and body-referenced attention; early and late sensorimotor learning; action guidance with internal and external cues; action execution; intention to act, imaginary movement, and current or expected sensory information from surroundings (Schu-botz & von Cramon 2003). Supplementary motor area, supplementary eye field and pre supplementary motor area control urge or prevention to act (Nachev et al. 2008).

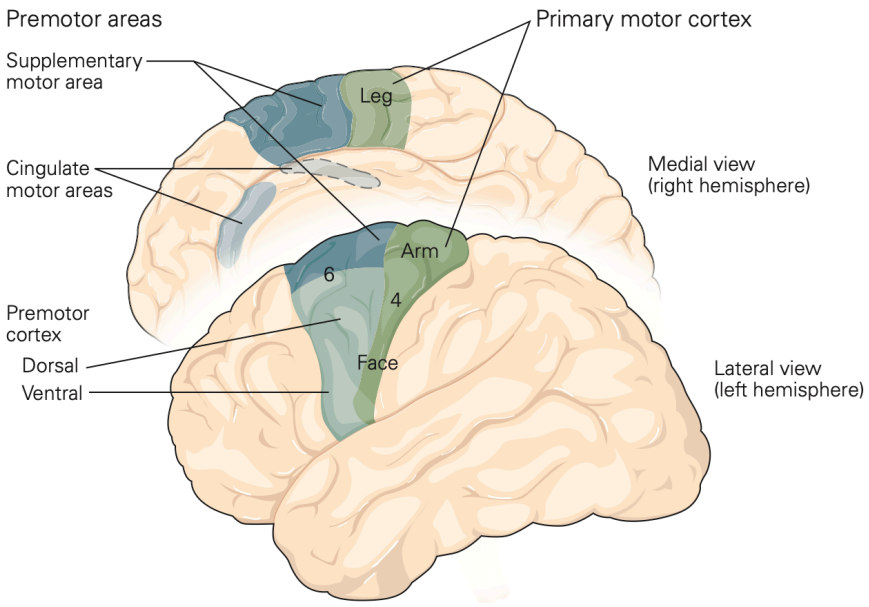

FIGURE 3. Cortical motor areas. Premotor cortex (Brodmann's area 6) is positioned laterally and consists of dorsal and ventral regions. Supplementary motor area is positioned medially superior to cingulate motor area. Primary motor cortex (Brodmann's area 4) is caudal to premotor cortex. (from Zagrean et al. 2013, 413)

3. NEUROPHYSIOLOGY OF ACUTE FATIGUE

In acute performance fatigue MVC force starts to decline caused by weakened efficiency of the muscles to contract and/or inadequate CNS drive to the motor units and muscle fibres (Gandevia 2001). Repeated activation of muscle fibres accumulates metabolites, disturbs perfusion and leads to force decrease, which is a result of spinal and/or supraspinal inhibition via activation of small-diameter afferents (Garland 1991), disfacilitation through reduced activity of large-diameter myelinated muscle spindle Ia-afferent fibers due to alternated intrinsic muscle mechanics and fatigued intrafusal fibres (Bongiovanni & Hagbarth 1990; Gandevia 2001; Heckman et al. 2008; Zhang & Rymer 2001), impaired muscle contraction and signal transmission, and decreased intra- and extracellular pH (Wilson et al. 1988). Declined contractile efficiency is compensated by increased signalling and/or recruitment of MUs (Kirsch & Rymer 1987). Lowering of the muscle fibre conduction velocity and mean motoneuron discharge frequency protects muscle fibres from premature peripheral fatigue and optimises input-output efficiency (Arendt–Nielsen et al. 1989; Gerdle & Fugl–Meyer 1992). MUs are recruited according to Henneman's size principle from smaller slow fatigue-resistant to large fast fatiguable ones (Henneman et al. 1965). Fatigue-resistant small MUs are frequently activated and their contribution to strength loss can be substantial during fatigue induced by submaximal contractions (Gandevia 2001; McNeil et al. 2011). Peripheral fatigue-induced changes are located in the axons of α-motoneurons, neuromuscular junction, along the sarcolemma, and in the transduction processes from sarcolemmal action potential to muscle fibre contraction (excitation-contraction coupling) (Sieck & Prakash 1995), and it is more profound at the early level of fatigue (Gandevia 2001). Central fatigue relates to changes in the activity of corticospinal and α-motoneurons, M1 cortex pre-motoneuronal neural circuits, and higher brain centers upstream from M1 cortex (Gandevia 2001).

Motor signal transmission may perturb in the muscle fibres, α-motoneurons, corticospinal motoneurons and M1 cortex pre-motoneuronal circuits (figure 4). From the dorsal horns of the spinal cord, where afferents synapse is a long-loop reflex pathway to brain stem, thalamus, somatosensory cortex and frontal brain areas (Mense 1983), and a short-loop reflex pathway to spinal motor circuits (Garland 1991), which modulates the excitability of α-motoneurons (Gandevia 2001). Excitability of α-motoneurons is also modulated by input from nearby α-motoneurons, and from the descending motor pathways from M1 cortex (corticospinal tract)

(Weavil & Amann 2018) and reticular formation of the brain stem (reticulospinal tract) (Duque et al. 2012). Corticospinal motoneurons and neural circuits at M1 cortex receives modulating input from sensorimotor areas: premotor areas, thalamus, basal ganglia and somatosensory areas (Zagrean et al. 2013, 24). Cerebellum participates in motor control modulation (Samii et al. 1997) via projections through brain stem. Afferent feedback from the muscle is integrated into the cerebral control of the motor signal, and it gives input to cognitive processes related to the perception of exertion and motivation (Nybo et al. 2014). Blocking afferent input decreases the maximal firing frequency of the MUs (Garland 1991). Activation of muscle spindle afferents increases muscle force and sensitivity to stretching, whereas group III/IV afferents decreases muscle force (Gandevia 2001). Supraspinal inhibition can be compensated by increasing motor drive, unlike spinal inhibition, that may be more limiting to performance (Garland 1991).

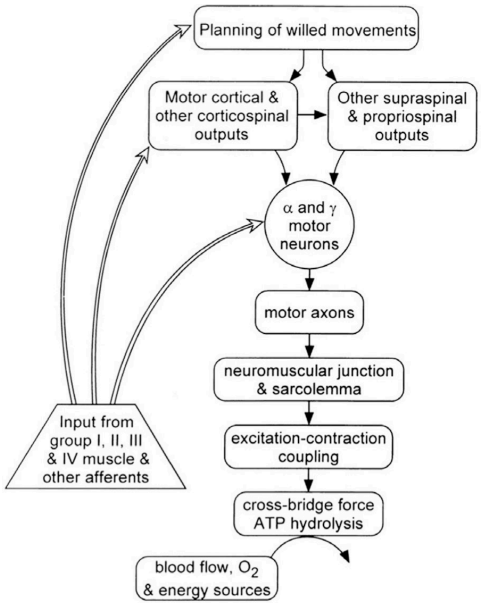

FIGURE 4. Signal transmission steps in voluntary contraction. (from Weavil & Amann 2018.)

3.1. Supraspinal and motoneuronal changes

Supraspinal pre-motoneuronal cortical neural circuits and corticospinal motoneurons can have acute fatigue-induced changes in excitability and motor output, which are driven by afferent feedback (Taylor et al. 2006) (figure 5).

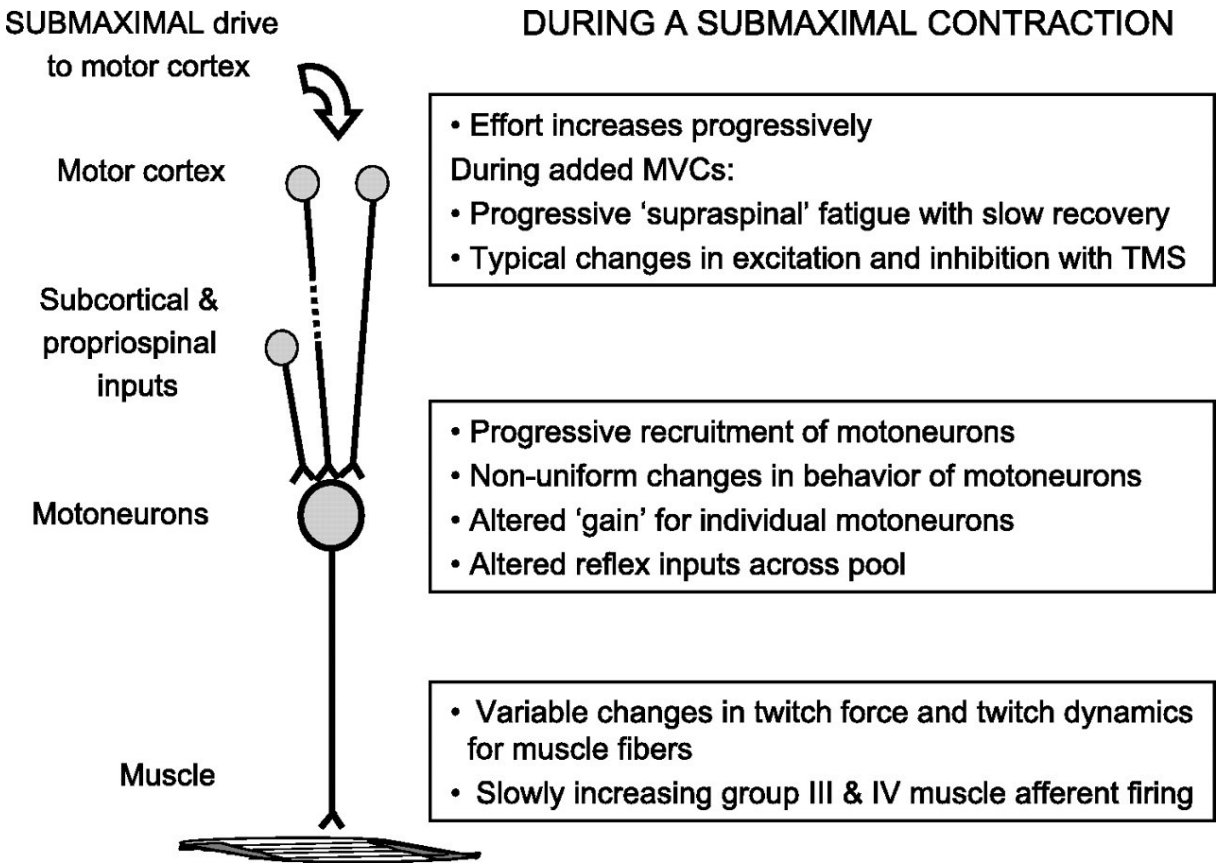

FIGURE 5. Factors of central fatigue during sustained submaximal contraction. (from Taylor & Gandevia 2008.)

Altered brain states and regional oxygenation have been connected to changes in power of rhythmic activity at distinct frequency bands of power spectrum from direct current potentials to 100Hz high-gamma activity (Robertson & Marino 2015). Increase of lower frequency (Paradiso et al. 2004) and α-band (7–14Hz) power is connected to state of inhibition and idling. α- activity is also linked to uninterrupted focus and attention, and it decreases during regional hypoxia (Périard et al. 2018). β- activity (13–30Hz) describes mental readiness and arousal (Périard et al. 2018) and α/β index suppressed arousal (Nielsen et al. 2001). Disinhibition of M1 cortex has increased simultaneously with relative decrease of frontal α- activity during incremental cycling test after respiratory compensation point (Robertson & Marino 2015).

Corticospinal excitability literature during contraction in fatigue have been gathered into table 1. During sustained MVC excitability of pre-motoneuronal circuits have shown to increase (Gandevia 2001) possibly as a compensatory mechanisms to reduced excitatory input to corticospinal pathway from short and long-latency reflexes (Duchateau et al. 2002). Fatigue-in-

duced modulation of M1 cortex excitability has been connected to corticocortical fascilitation and/or disinhibition from premotor areas and prefrontal cortex (Robertson & Marino 2015), afferent feedback through somatosensory cortex, premotor cortex, supplementary motor area, prefrontal cortex, basal ganglia, cerebellum and thalamus (Jiang et al. 2012; Jiang et al. 2016; Taylor et al. 2006) and motivation for the current task (Sidhu et al. 2018).

TABLE 1. Corticospinal excitability modulation during contraction in fatigue.

Reference	Protocol	Result
(Hoffman et al. 2009)	N=10. In brief isometric plantar flexion at 80, 90, and 100%MVC and 30%MVC during sustained contraction at 30%MVC.	↑ MEP/$Mmax_{0\%\ failure}$ and MEP/$Mmax_{100\%\ failure}$ (SOL and medial gastrocnemius) ↑ CMEP/$Mmax_{0\%\ failure}$ and CMEP/$Mmax_{100\%\ failure}$ (SOL and medial gastrocnemius) at 30%MVC, ↔ MEP/oMmax and CMEP/oMmax (SOL) at 30%MVC ↔ between MEP/$Mmax_{0\%\ failure}$ and MEP/$Mmax_{100\%\ failure}$ (SOL and medial gastrocnemius) at 80, 90, and 100%MVC, ↔ between CMEP/$Mmax_{0\%\ failure}$ and CMEP/$Mmax_{100\%\ failure}$ (SOL and medial gastrocnemius) at 80, 90, and 100%MVC.
(Iguchi & Shields 2012)	N=10. In brief maximal and 10-s at 10%MVC (following every 9th MVC) isometric plantar flexions after 7sec/r3-s contraction x 9 trials x 5 sets/r10-s.	↑ MEP (SOL) at 10%MVC.
(Keller et al. 2011)	N=29. During brief maximal isometric elbow flexion after sustained contraction at 20%MVC.	↑ MEP/blMEP (no change in Mmax) (biceps brachii) at MVC during task failure and recovered to baseline within 5 min, ↑ MEP/blMEP (no change in Mmax) (biceps brachii) at 20%MVC.
(Kennedy et al. 2016)	N=9. In 2-min sustained maximal isometric knee extension and during brief MVC after sustained MVC.	↑ MEP/cMmax (vastus lateralis) during and after sustained MVC, ↔ TMEP/cMmax (vastus lateralis) during and after sustained MVC.
(Kirk et al. 2019)	N=16. In 3-s maximal isometric plantar flexions after max repetitions of 3-s/r2-s x 6 sets/r90-s at 85%MVC.	↓ MEP/cMmax (SOL) at MVC and recovered within 10min.
(Klass et al. 2008)	N=11. During sustained isometric elbow flexion at 20%MVC.	↑ MEP/cMmax (biceps brachii) at 20%MVC.
(McNeil et al. 2011)	N=8. During 10-min sustained isometric elbow flexion at EMG level of fresh muscle force at 25%MVC.	↓ CMEP/sameMmax (biceps brachii) at EMG (25%MVC), Similar ↓ MEP/sameMmax and CMEP/sameMmax (biceps brachii) at EMG (25%MVC) during cortical SP.
(Ruotsalainen et al. 2014)	N=11. In brief maximal isometric elbow flexion in hypertrofic exercise with total 13 repetitions x 3 sets consists of 8 free weight, 5 isokinetic+isometric elbow flexion movements.	↑ MEP/cMmax (biceps brachii) at MVC. Progressive decline from the beginning of the exercise till the end as fatigue accumulated.
(Smith et al. 2007)	N=8. In brief maximal and 5%MVC isometric elbow flexion during 70-min sustained contraction at 5%MVC.	↑ MEP/sameMmax (biceps brachii and brachioradialis) at 5%MVC, ↔ MEP/sameMmax (biceps brachii and brachioradialis) at MVC.
(Szubski et al. 2007)	N=12. In 90-s sustained maximal index-finger abduction in norm- and hyp-oxia.	↑ MEP/cMmax (first dorsal interosseus muscle) in normoxia and hypoxia at MVC.
(Søgaard et al. 2006)	N=9. In brief MVC and 15%MVC isometric elbow flexion during 43-min sustained contraction at 15%MVCs.	↑ MEP/sameMmax (biceps brachii and brachioradialis) at 15%MVC, ↔ MEP/sameMmax (biceps brachii and brachioradialis) at MVC.

MEP = motor-evoked potential, TMEP = thoracic MEP, blMEP = baseline MEP, cMmax = concomitant Mmax, sameMmax = same condition Mmax, oMmax = approximated ongoing Mmax from 0 and 100% of time to task failure

Fatigue-induced intracortical $GABA_B$ mediated M1 cortex inhibition during sustained submaximal and maximal contraction has been shown to increase when measured with long-interval paired-pulse TMS stimulus (long-interval intracortical inhibition, LICI) (Gruet et al. 2013; McNeil et al. 2009; McNeil et al. 2011). Another measure of cortical and spinal $GABA_B$ mediated inhibition, cortical silent period (SP), the period of attenuated EMG activity after TMS-induced MEP (McNeil et al. 2011; Škarabot et al. 2019) has shown to increase during intermittent (Benwell et al. 2007; Iguchi & Shields 2012) and sustained MVC (Taylor et al. 1999), remain unchanged during brief contractions from 50 to 100%MVC after fatiguing cycling exercise (Jubeau et al. 2017) and decrease during brief MVC after fatiguing submaximal intermittent contractions (Kirk et al. 2019). Different results might be related to reperfusion and clearance of metabolites during rest periods that leads to reduced III/IV afferent activity (Kirk et al. 2019). Higher force levels and rebounding force after stimulus have shown to shorten cortical SP (Mathis et al. 1998; Matsugi 2019). Cortical SP is increased in fatigued but not in unfatigued muscle with prolonged group II/IV afferent activity (Kennedy et al. 2016), and fentanyl blockage of group III/IV afferent activity has lead to shortened cortical SP (Sidhu et al. 2017). It is suggested that LICI and cortical SP share distinct inhibitory circuits, both consists of spinal inhibitory component and are not only limited to intracortical inhibition (McDonnell et al. 2006).

Excitability of axons of corticospinal motoneurons during fatigue has been reported to reduce (Butler et al. 2003; Finn et al. 2018; Martin et al. 2006; McNeil et al. 2009; McNeil et al. 2011), show no change (Hoffman et al. 2009; Kennedy et al. 2016) or increase (Hoffman et al. 2009). Contradicting results might be explained by differences between studies related to control of motor drive from M1 cortex (Duchateau et al. 2002; Finn et al. 2018; McNeil et al. 2011) and the type and size of recruited corticospinal motoneuron populations (Finn et al. 2018). While not directly related to fatigue, temporal summation of descending TMS-induced volleys might change with increased signal conduction time from M1 cortex to muscle (Andersen et al. 2003). M1 cortex drive to motoneurons is affected by efficiency at corticomotoneuronal synaptic transmission, which has shown to decrease during post-contraction depression at rest and during small activation after sustained MVC (Gandevia et al. 1999; Petersen et al. 2003). Excitability of axons of corticospinal motoneurons recovers faster than cortical pre-motoneuronal circuits and also leads to earlier facilitation (Gandevia et al. 1999).

Increased excitability of pre-motoneuronal circuits enables recuitment of corticospinal motoneurons with decreased responsiveness and larger fresh motoneurons with higher discharge frequency. Increased inhibition prevents repeated discharge of neurons, optimises activation patterns, synchronizes information transfer between neural circuits and spatially controls which neural pathways are available for activation (Heckmann et al. 2008). Inhibition also modulates the relation between sense of effort and motor output strength (de Morree et al. 2012). Spinal and cortical mechanisms compensate each other during different phases of fatigue. Longer recovery period of cortical excitability during rest is compensated by earlier facilitated state of corticospinal motoneurons after post-contraction depression. As fatigue progress, more control from automatic processes is shifted to higher levels of corticospinal pathway, where information is broadly integrated and reserve for increased motor output is still available.

3.2. Motor unit activity during fatigue

After sustained MVC axons of recruited α-motoneurons are hyperpolarized, which increases their discharge threshold and leads to hypoexcitability that is largest immediately after contraction (Vagg et al. 1998). MU firing frequency decreases in the beginning of an intense contraction with increased recurrent inhibition and muscle spindle disfacilitation (Bigland–Ritchie et al. 1986; Gandevia 2001). Activity-dependent changes in α-motoneurons intrinsic properties modulate frequency-adaptations (Gandevia 2001), which are more common in larger easily fatiguable high frequency α-motoneurons (Spielmann et al. 1993).

Cross-bridge formation between muscle fibre filaments depends on muscle fibre length and calcium dynamics in the muscle filament compartments. Fatigue is more severe at optimum muscle lengths when 1) the area between filaments to form cross-bridges is maximised (Fitch & McComas 1985), and 2) ATP-dependent calcium release and clearance is high. The more severe fatigue is, the more dominant deficient in calcium handling becomes relative to impairment in cross-bridge function (Lännergren & Westerblad 1991).

Fatigue related changes in neuromuscular junction and muscle fibre membrane conductivity. Muscle fibre conduction velocity and rate of force development (RFD) increases with muscle temperature (Murakami et al. 2014). Maintaining ion and neurotransmitters homeostasis du-

ring fatigue consumes energy and time. Fast-twitch fatiguable motor units are more vulnerable to reduced synaptic efficacy in neuromuscular junction. Presynaptic failures include a propagation blockage of action potentials via axons or reduced secretation of neurotransmitters in the presynaptic terminal. (Sieck & Prakash 1995.) Increased extracellular potassium concentrations and inactivation of the sodium channels decreases sarcolemmal excitability (Piitulainen et al. 2008; Piitulainen et al. 2012; Sieck & Prakash 1995); whereas low pH maintains excitability (Pedersen et al. 2005), but decreases conduction velocity (Juel 1988).

3.3. Changes in cerebral neurotransmission, metabolism and blood flow

EEG measures electrical brain activity that is caused by electrical field of ion currents in the post-synaptic terminals, dendrites and cell bodies; and extracellular volume. Transduction converts movement of neurotransmitters between synapses to activation of ion channels (Purves et al. 2018, 85). Transmitter interaction is restricted to specific brain regions and neural pathways. Animal studies have shown that many neurotransmitters dopamine (DA), serotonin (5-HT), acetylcholine and norepinephrine (NE) acts as modulators of corticospinal motoneurons excitability through voltage-sensitive sodium and calsium persistent inward currents (PICs) in the neuron the dendrites and soma (Lee & Heckmann 1999). PICs are critical in several-fold amplification and attenuation of synaptic input, self-sustained firing of the motoneuron induced by short input, increased polarisation after firing relative to onset voltage, and temporal summation of excitation eventually leading to saturation. (Heckman et al. 2008.)

Serotonin. 5-HT modulates the release of many hormones (Cordeiro et al. 2017) and increases cerebral heat storage (Soares et al. 2004). 5-HT is synthesised from free-tryptophan, that increases during fatigue. In rats, increased serotonergic activity inhibits performance, whereas reduced serotonergic activity increases endurance performance. In humans 5-HT uptake inhibitor citalopram decreased CSE by increasing motor threshold, latency, cortical SP and $GABA_A$ mediated short interval intracortical inhibition (Robol et al. 2004). Many of the results in animal studies have not been replicated with humans, which might be related to different roles of 5-HT and other neurotransmitters in humans. (Cordeiro et al. 2017.)

Adenosine. Adenosine has mostly inhibitory, but also minor excitatory role on neurotransmission, and acts as an important vasodilator. Adenosine increases when high-energy phosphate

bonds are detached from ATP, and ratios of ADP and AMP relative to ATP starts to elevate. (Latini & Pedata 2001.) Ingestion with adenosine antagonist caffeine increased CSE and VA at rest, but not at task failure compared to control during single-leg knee extension exercise (Bowtell et al. 2018).

Norepinephrine. NE is a neurotransmitter related to motivation, motor behaviour, arousal, consciousness, reward mechanism (Meeusen et al. 2006), increased heart rate, release of 5-HT, and it also has a hypothermic effect. NE increases during moderate exercise, and it is synthesized from amino acid tyrosine or dopamine. Noradrenergic pathways project from brain stem to hypothalamus, thalamus, hippocampus, limbic system and cerebral cortex. (Berridge & Waterhouse 2003; Meeusen et al. 1997; Roelands & Meeusen 2010.) NE decreases performance (Klass et al. 2012; Roelands & Meeusen 2010), voluntary activation, and psychomotor vigilance, and increases supraspinal inhibition (Klass et al. 2012). It has been shown with cats, that NE increases bistable activation of spinal motoneurons, which enables self-sustained firing or inhibition to brief synaptic inputs (Lee & Heckman 1999). In humans NE reuptake inhibitor reboxetine increased CSE (Plewnia et al. 2002).

Dopamine. DA is related to control of movement, perceived exertion, motivation and reward (Cordeiro et al. 2017). DA increases during exercise in animals (Foley et al. 2008) and with humans during running in heat (Wang et al. 2000; Zhao et al. 2015) and playing hand controlled video game (Koepp et al. 1998). Low DA concentrations are linked to termination of an exercise (Bailey et al. 1993). DA agonism during exercise in normal temperature increases core temperature and decreases or stalls RPE (Jacobs & Bell 2004; Meeusen et al. 1997). 5-HT (Bailey et al. 1993; Cordeiro et al. 2017) and adenosine (Myers & Pugsley 1986) inhibit DA. DA activity at substantia nigra pars compacta facilitates M1 cortex through thalamus (Foley & Fleshner 2008), and striatal ramping activity is connected to temporal information processing during movement preparation (Emmons et al. 2017) as in RP (Fifel 2018).

Glucose availability. During hypoglycemia and exhaustive exercise, glycogen decreases in the cerebellum, cortex, hippocampus, brain stem and hypothalamus (Matsui et al. 2011), areas related to locomotion, metabolism, motor control and arousal (Matsui et al. 2019). At exhaustion, brain maintains ATP and PCr levels, contrary to muscle, where they decrease (Matsui et al. 2017). Carbohydrate ingestion during fatigue reduces 5-HT accumulation (Nybo et al.

2003) and drop in VAL (Nybo 2003), and momentally increases immediate CSE and MVC without changes in TMS elicited superimposed twitch force (Gant et al. 2010). Astrocytic glycogenolysis synthesizes ATP and lactate, and maintains K+ homeostasis, and it is stimulated by NE and 5-HT (Matsui et al. 2017). Glycogen is oxidized or converted into lactate that is shuttled into neurons to preserve blood glucose (Matsui et al. 2017) or released into blood and perivascular fluid (Dienel & Rothman 2019).

Cerebral blood flow and hyperthermia. Cerebral blood flow (CBF), measured as a middle cerebral artery mean blood velocity (MCA Vmean), provides substrates, and removes metabolites, neurotransmitters and heat. It is modulated by arterial carbon dioxide (PaCO2) and oxygen tension (PaO2), blood pressure (Pb), and neural activity. (Nybo & Secher 2004.) In the beginning of exercise, CBF elevates and remains constant during low-intensity exercise, but may decrease in hyperthermia (Nybo & Nielsen 2001a) or due to rapid changes Pb (Perry et al. 2014). Although CBF is mostly unaltered during exercise, there exists no-oxygen-dependent changes in regional blood flow (Nybo & Secher 2004). Relatively stable cerebral metabolic rate for oxygen during exercise (Vafaee et al. 2012) increases during hyperthermia (Nybo et al. 2002) and recovery after maximal exercise (Ide et al. 2000), and is not jeopardized by substantial decreases in MCA Vmean and oxygen delivery (Hansen et al. 1986).

Cerebral oxygen consumption drives cerebral heat production, and lack of structures generating mechanical work (Yablonskiy et al. 2000) elevates cerebral tissue temperature higher than core during rest and exercise (Nybo & Secher 2004). CBF has a cooling effect, if there is a sufficient temperature difference between arterial blood and cerebral tissue (Nybo & Secher 2004). Rise in cerebral temperature, especially in the hypothalamus inhibits long duration physical performance (Fortney & Vroman 1985), and its strength is modulated by sensory feedback (Nybo & Secher 2004). Surprisingly short duration performance increases in heat (Yamaguchi et al. 2020). In hyperthermia, VAL decreases in fatigued and non-fatigued muscles during sustained MVC, but not during intermittent MVC, without differences in total force development between hyperthermic and normothermic environments (Nybo & Nielsen 2001a). Similar increase in CSE during fatiguing sustained MVC has been shown in hyperthermic and normothermic environment (Todd et al. 2005).

3.4. Rating of perceived exertion

Perceived exertion is defined as perception of heaviness, strain, effort, pain, discomfort, and fatigue related to physical work (Robertson & Noble 1997), and it is measured on numeric scales (rating of perceived exertion, RPE) RPE 6–20 and OMNI RPE 0–10. RPE is a conscious measure of psychophysiological stress (figure 6) from light intensity to maximal exertion, and it has a linear relationship between workload and heart rate. Physiological stress mediators are ventilation, pH, oxygen consumption, temperature and fatigue and psychological factors include motivation, experience of similar situations, information related to current performance, and exercise-induced pain. (Haile et al. 2015, 15–16.) Perceived exertion optimises power output and metabolic rate to protect muscles and organs from premature operating and/or structural failures.

In non-fatigued state, RPE increases with rate of force development, force error, frontal-central late RP amplitude, mismatch between force and anticipated effort, attention or effort related to force control (Slobounov et al. 2004). Force magnitude has shown positive (de Morree et al. 2012) and no effect on RPE (Slobounov et al. 2004).

Working at constant RPE and duration, the intra-session power output progressively decreases, but the mean power output between sessions stays similar. (Gibson et al. 2006.) At moderate-work levels RPE is modulated by the expectancy of task duration (Rejeski & Ribisl 2016) and rate of increase in RPE has shown to predict exercise duration (Crewe et al. 2008). According to ”reafferent corollary discharge” theory, RPE is an integration of increased reflex input caused by increased muscle recruitment, and effort related to motor drive (de Morree et al. 2012). RPE could be the result of comparison between predicted and actual afferent feedbacks (Abbiss et al. 2015). Cerebral facilitation by peripheral feedback is thought to result in reduced cerebral oxygen to carbohydrate+lactate uptake ratio and maximal RPEs (Dalsgaard et al. 2002). Elevated plasma glucose levels increases power output without changes in RPE (Ali et al. 2017). Effort describes how much mental and physical energy work consumes (Abbiss et al. 2015) and it may be maximal when exertion is submaximal (Dalsgaard et al. 2002), especially during short work period (Swart et al. 2012).

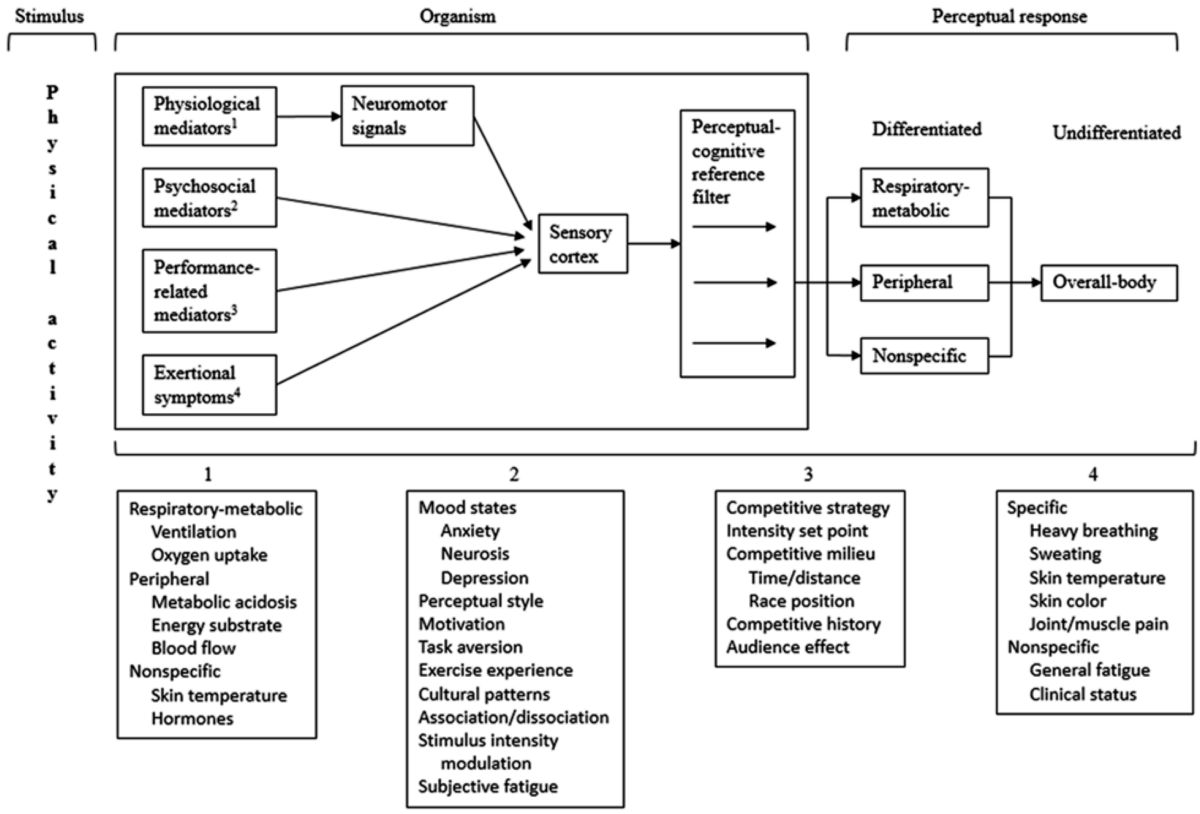

FIGURE 6. Rating of perceived exertion is a result of physiological, psychosocial, performance-related and symptomal exertional mediators. (from Haile et al. 2015.)

RPE originates from motor control and emotions related areas (de Morree et al. 2012). RPE increase during fatigue is associated with increased cognitive effort related to planning of actions (Berchicci et al. 2013), interrupted focus and attention and lowered level of mental readiness and arousal (Nielsen et al. 2001; Périard et al. 2018), earlier RP onset (Berchicci et al. 2013), increased central RP amplitude (Berchicci et al. 2013; Slobounov et al. 2004), unchanged frontal-central RP amplitude (de Morree et al. 2012), decreased central RP amplitude and VAL (Spring et al. 2016). RPE is unchanged despite increases in power output during cycling, when transcranial direct current stimulation is applied on dorsolateral prefrontal cortex (Lattari et al. 2018).

4. PREMOTOR BRAIN ACTIVITY DURING FATIGUE

In the reviewed literature, the view on modulation of RP during fatigue is non-consistent. This might be partly explained by differences in methods and fatigue protocols. RP components are measured online and offline in varying spatial locations and time windows relative to force/ EMG onset. Both isometric or dynamic and maximal or submaximal and lower or upper body intermittent single limb contractions have been used (table 2).

TABLE 2. Readiness potential modulation by fatigue, effort and force.

Reference	Protocol	Result
(Bechicci et al. 2013)	n=18. Online during knee extension at 40%MVC divided into 60 trials x 4 blocks with <2-min inter-block rest	↑ late RP AMP (vertex) in high and low effort cohorts, ↑ early RP AMP (contralateral precentral) in high effort cohort, ↓ prefrontal positivity latency in high effort cohort
(de Morree et al. 2012)	n=16. Offline during 50 dynamic unilateral elbow flexions with fatigued and non-fatigued arms at 20 and 30% of 1RM. Fatiguing task consisted of ~56 maximal eccentric elbow flexions.	↔ RP AMP with ↑ fatigue ↑ RP AMP (midline frontal), but ↔ RP AMP (contralateral and ipsilateral central) with ↑ weight
(Freude & Ullsperger 1987)	n=9. Online during isometric 150–250 monospike handgrip contractions at 20, 50 and 80%MVC.	↑ RP area (vertex) in fatiguing 80%MVC and non-fatiguing 20% MVC, ↓ RP area (vertex) in non-fatiguing 50%MVC
(Johnston et al. 2001)	n=6. Online during isometric graspings at 70%MVC divided into 4-s contraction x 40 trials x 3 blocks.	↑ early RP AMP (midline precentral, central and parietal), ↑ early RP AMP (vertex) was larger than central contralateral and ipsilateral with an effect of block, ↑ RP AMP (precentral midline) with an effect of block, ↑ late RP AMP (central contralateral) with an effect of block
(Liu et al. 2005)	n=8. Online during maximal grip task divided into 2-s contraction x 40 trials x 5 blocks with inter-trial interval of 5-s.	↔ RP peak negative potential AMP (midline precentral, central and postcentral; contralateral and ipsilateral central)
(Shibata et al. 1997)	n=10. Online during isometric elbow flexions at 20%MVC. Three separate tasks: 50 short contractions, 2-s contraction x 50 trials and 2-s contraction x 5 trials x 10 sets/r30-s with occlusion.	↑ late RP AMP (contralateral central and vertex) relative to ipsilateral RP AMP in all tasks, ↓ late RP AMP (contralateral central) with occlusion relative to other tasks
(Slobounov et al. 2004)	n=6. Online during 60 isometric index finger contractions at 30, 50 and 50%MVC with RFD of 60–70%MVC/s.	↑ late RP AMP (precentral and vertex) with ↑ RFD and ↑ anticipated effort related to force production, ↓ late RP AMP (precentral and vertex) with ↓ anticipated effort related to force production
(Spring et al. 2016)	n=16. Offline during 60 dynamic knee extension at 20%MVC. Fatiguing task consisted of combined 30-min at 60%MAP and 10-km all-out time trial cycle ergometer work (n=16) with 15-min rest between.	↓ RP AMP (bilateral precentral and contralateral central)

AMP=amplitude, MAP=maximal aerobic power, RFD=rate of force development, RP=readiness potential, r30-s=inter-set rest of 30-s, SOL=soleus

Berchicci et al. (2013) and Johnston et al. (2001) have shown increased late RP amplitude during fatiguing submaximal isometric exercise, whereas de Morree et al. (2012) found no signi-

ficant effect. In contrast, Spring et al. (2016) have shown decreased RP amplitude after fatiguing exercise, especially in the contralateral early component. Contralateral late RP amplitude has been shown to decrease with occlusion during fatigue (Shibata et al. 1997). RP area has been shown to increase during non-fatiguing and fatiguing rhythmical isometric handgrip contractions at 20 and 80%MVC, respectively. RP area reduced during non-fatiguing contractions at 50%MVC where fatiguing task was speculated to require more cognitive effort, whereas non-fatiguing task at 20%MVC required more skill. Decreased RP area during 50%MVC was seen as a lack of attention and motivation to the monotonic task. (Freude & Ullsperger 1987.) Reduced VAL correlates modestly (r=0.64, n=16) with decreased RP amplitude during fatigue (Spring et al. 2016).

Increase in RFD increases RP amplitude (de Morree et al. 2012; Slobounov et al. 2004), whereas during fatigue, late RP amplitude decreases with RFD (Shibata et al. 1997). Slobounov et al. (2004) modified force trace feedback, so that actual force produced (30%MVC) was displayed with exaggerated force trace (70%MVC) and vice versa. Maintaining the higher force trace was perceived more effortful and resulted in larger late RP amplitude, suggesting that RP was not modulated by force level per se. High RPEs have been connected to earlier RP and larger prefrontal positivity (Berchicci et al. 2013) (figure 7). Force level on the other hand has shown positive (de Morree et al. 2012) and no effect (Slobounov et al. 2004) on RP amplitude.

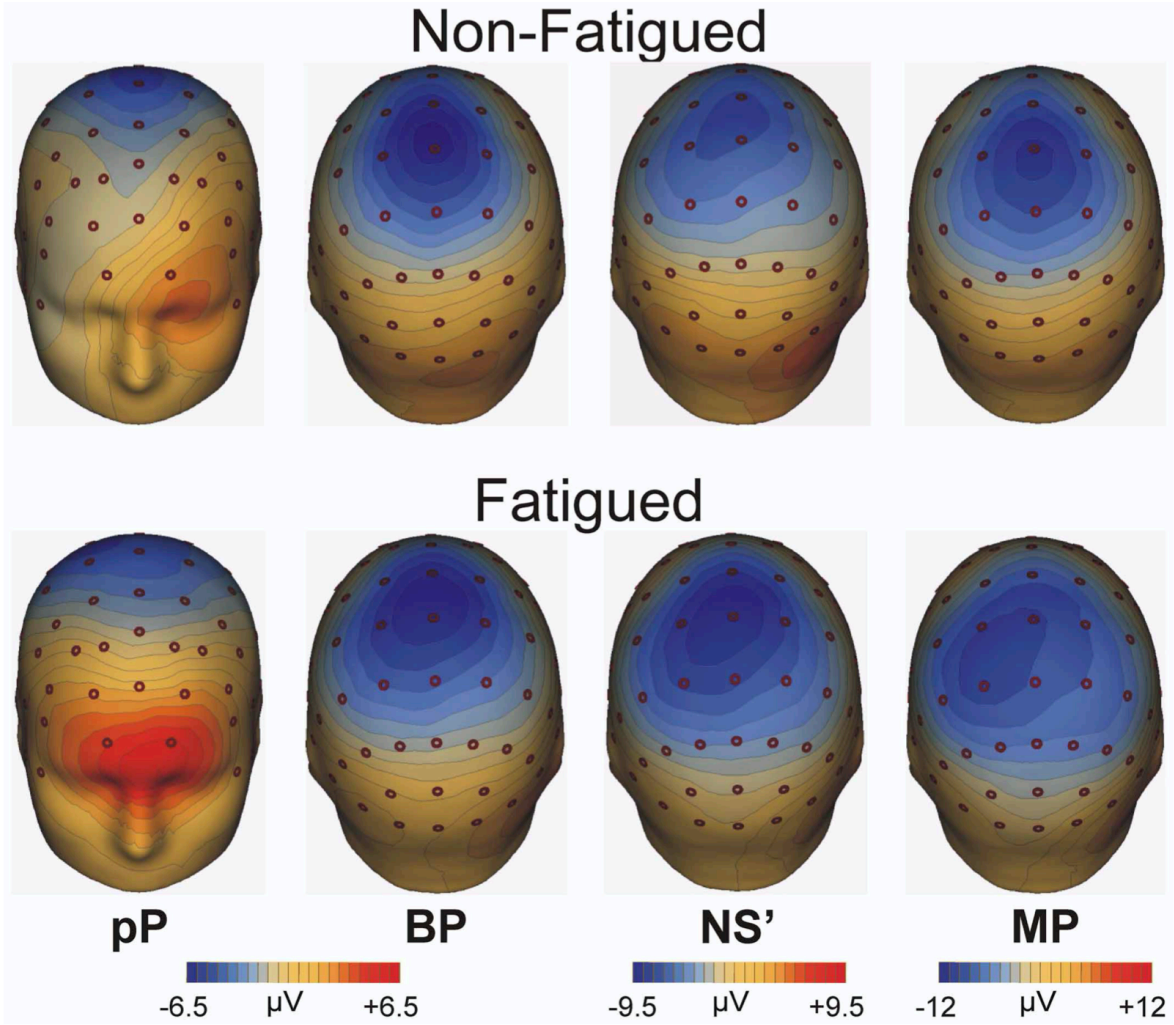

FIGURE 7. Topographical map of movement related cortical potential components grouped by perceived exertion into non-fatigued and fatigued. Time windows for prefrontal positivity (pP) from -700 to -200-ms, RP from -1000 to -500-ms, NS' from -400 to -100-ms and MP from -100-ms to force onset. (from Berchicci et al. 2013.)

5. PURPOSE OF THE STUDY

The purpose of the study was three-fold.

1) The purpose was to investigate premovement activity measured as RP during fatiguing lower body work, and if the possible changes in its amplitude are related to CSE, VAL and perceived exertion.

2) The purpose was to investigate if change in RP amplitude increases in the beginning of the fatigue and then decreases as fatigue progresses.

3) The purpose was to investigate the source of the reduced negative non-slope-dependent RP amplitude. This may be caused by larger proportion of positive slope shifts during fatigue. Other explanations might be larger positive amplitudes or smaller negative amplitudes.

Current literature shares non-consistent view on fatigue-induced modulation of RP (table 2). This is the first study to investigate the impact of fatigue on distribution of negative and positive RP shifts.

6. METHODS

6.1. Participants

A total of 10 healthy male volunteers (29.8±7.4 years) with a variable training background in soccer, track and field, CrossFit, ice hockey, triathlon, downhill skiing and racquet sports were recruited for the study. Subjects did not have any injury history for the past six months and any past neurological disorders acted as a disqualification criteria. Procedures and handling of the privacy data was informed to the subjects beforehand and they had to give their written consent of approval. Subjects also filled a leg dominance survey. Three subjects had a preference for the left leg and seven for the right leg. The dominant leg was used in the tests. Subjects were instructed to avoid any fatiguing exercise 24-h prior to testing sessions. Subjects had the right to cancel the experiment at any time point. The study was approved by the university of Jyväskylä ethics committee.

6.2. Study design

Measurements were done at biomechanics laboratory of Neuromuscular Research Center of Biology of Physical Activity discipline within the faculty of Sport and Health Sciences at University of Jyväskylä during 20.3.–1.6.2019. Each subject participated in a familiarisation and two fatigue sessions. One of the fatigue sessions worked as a control and the order of the sessions were randomised so that half of participants started with control and half with fatigue session.

Familiarisation session consisted of MVC assessment, TMS familiarisation and 10 fatigue repetitions. Fatigue repetitions were self-started during a 10-s time window following a beep sound every 20-s. Subject elevated torque to 50%MVC for 4-s. Before starting producing torque subject was instructed to hold breath for few seconds and avoid any muscle activations and eye blinking. After torque had started to elevate subjects could discard restrictions. EEG was recorded during fatigue repetitions. Signal quality was inspected offline and feedback about the torque producing technique was given to the subject.

Fatiguing sessions started with the following measurements: MVC assessment, Mmax, TMS hotspot and CVAL intensity. Recruitment curve was measured two times before and after fatiguing protocol. VAL and RPE was measured before, between and after fatiguing blocks. Fatiguing sessions included two 30 repetition blocks for a session total of 60 repetition. EEG was recorded during repetitions. During fatiguing block each repetition started with a 4-s force production at 50%MVC. This was followed by an immediate MVC for 3-s. The start and stop of the MVC was announced by the measurer. Subject was verbally encouraged during MVCs. In the control block force was maintained at 10%MVC for 7-s.

MVC used for relative torque levels was measured at the beginning of the session and remained fixed for all protocols except during VAL assessment where first trial was used as a reference MVC. EEG cap was disconnected from the amplifier before the last repetition of the fatigue block to allow disturbance-free use of cortical TMS during MVC part of the contraction.

6.3. Measurements

Timing of the trials was controlled by a timer displayed on a screen front of the subject combined with a beep tone during interval change. TMS intensity was controlled manually with computer. TMS was automatically triggered with computer when torque reached plateau at the current target torque level.

6.3.1. Plantarflexors torque measurements

Subjects were seated in an ankle dynamometer (Neuromuscular Research Center, University of Jyväskylä) (figure 8). Hip angle was set to 120°, knee angle to 180° and ankle angle to 90°. Straps were used to attach the dominant leg ankle to the dynamometer pedal and thigh above knee to the bench. Torso and waist were also attached to the bench with race car type safe belts. The pedal had a rotational axis that was positioned under the heel and dynamometer measured torque. Contractions were done isometrically. A/D converter (CED Power1401 mk II; Cambridge Electronic Design Ltd, Cambridge, UK) was used to sample torque signal at 4kHz.

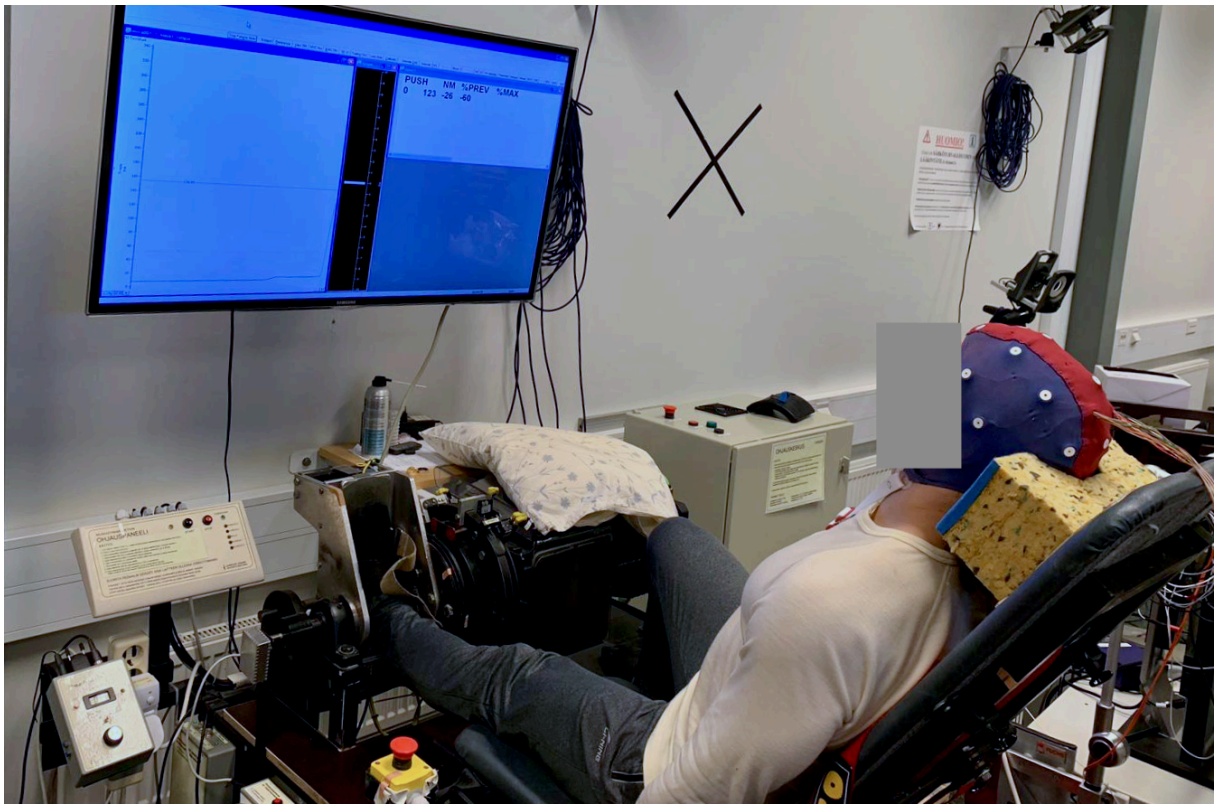

FIGURE 8. Ankle dynamometer was used to measure plantarflexors torque.

MVC measurements consisted of warm-up trials at 50%, 70% and 90% of maximal effort for 3-s each with a 20-s rest between trials. After 30-s of the last warm-up trial subject performed 2–5 MVCs until torque did not increase more than five percent. There was a 1-min rest between each MVC trials. Subjects were encouraged until torque achieved plateau or started to decline. Maximum value of the trials was used as the MVC. Subject were instructed to push the pedal with the ball of the foot and whole body was allowed to use in support of force production.

6.3.2. Electromyography

Surface EMG was measured from the soleus (SOL) and tibialis anterior (TA) with self-adhesive Ambu BlueSensor N-00-S Ag/AgCl ECG electrodes with diameter of 33 x 22mm (Ambu A/S, Ballerup, Denmark). SENIAM recommendations were used for the skin preparation and electrode locations. Skin was shaved, scraped with sandpaper and cleansed with disinfectant solution. Electrode–skin impedance was checked to be under 2kΩ for bipolar and under 4kΩ for the pseudomonopolar connections. In the pseudomonopolar SOL connection both electro-

des were placed into Achilles tendon according to Hadoush et al. (2009). One electrode was placed 2cm distal to the insertion of the medial gastrocnemius muscle and the second 3cm medially and 2cm superiorly to medial malleolus. In the bipolar TA connection electrodes were placed into proximal third of the line from tip of the fibula into the medial malleolus with a interelectrode distance of 2cm. Reference electrode for both connections was placed to medial malleolus. Pulling of the wires was removed by taping the wire near electrodes on the skin.

EMG signals were preamplified by a gain of 100 for measurements including DS and by a 1000 for all the rest. Signal was high-pass filtered at 10Hz with Digitimer NL824 (Digitimer, Welwyn Garden City, UK). Then signal was bandpass filtered at 0.01–1kHz with a differential amplifier (NL900D/NL820A; Digitimer, Welwyn Garden City, UK), galvanically differentiated, A/D converted (CED Power1401 mk II; Cambridge Electronic Design Ltd, Cambridge, UK) and sampled at 5kHz on a computer with a Spike2 software (v4.11; Cambridge Electronic Design Ltd, Cambridge, UK). EMG signal quality was assessed during rest to have a mean of absolute under 10μV for both connections.

6.3.3. Transcranial magnetic stimulation

A paper grid of 9x9 points separated by 5mm with orientation guidelines was placed over the EEG cap. Center of the paper was aligned with the vertex. Each point was labeled by its row and column number from one to nine. Grid was shifted by the length from the edge of the coil to the coil center and tilted 30° relative to sagital plane. Coordinate pair (3, 3) corresponded the vertex.

Magstim 200 and Bistim TMS stimulator units (Magstim, Dyfed, UK) were connected together, and a double-cone coil (2x126mm in diameter) was used to deliver single monophasic rectangular pulse of width 1 ms to the dominant leg ankle plantarflexors motor representation area at M1 cortex. TMS pulse intensity and timing was controlled semi-automatically by computer.

In the active measurements the plateau of the ankle torque triggered the TMS stimulus. A randomised delay from 1–1.5-s to the stimulus onset was added after the plateau detection.

Motor hotspot measurement. Cortical motor hotspot for TMS was searched during activation of 20%MVC. Subject followed timer displayed on the screen to start producing torque. A target torque meter was shown on the screen and system was set to trigger stimulus when the right target torque had reached plateau at the correct torque level. Subject was instructed to relax immediately after the stimulus. Torque producing efforts followed in clusters of four separated by 10-s and with inter-effort rest of 6-s. For the stimuli stimulator intensity was first set to 50% of maximal stimulator output (SMO) to elicit clear visually inspected MEP. Computer kept track of each grid points peak and mean peak-to-peak MEP values. Points were sorted ascending by response amplitude. The point location of the stimulus was inputted by the user. TMS coil was handheld by fixing the target of the coils edge on the grid points. Coil was rotated in the transverse plane by 30° to the sagital plane. In each selected grid point TMS was applied two times at the current stimulator intensity. TMS was first applied on the vertex at the grid point of (3, 3). Then the next corresponding column of points were stimulated until MEP started to decline. The row of points corresponding to biggest MEP was then chosen. Then the point of maximum MEP and the surrounding eight points were chosen and stimulator intensity was decreased by 1–5% depending on the maximum MEP amplitude. All the nine points were stimulated and again the point corresponding maximum MEP was chosen. This cycle was repeated until all the least excitable points could be ruled out. If there were two competing points the hotspot was marked between them. On average 30–50 stimuli was used to locate the hotspot.

Active motor threshold measurement. MTAT program (Motor Threshold Assessment Tool v. 2.0, ClinicalResearch.org) was used to define an active motor threshold (AMT). Program prescribed stimulator output intensities based on previous MEP responses. Response was qualified as a MEP if time window from 25 to 75-ms relative to stimulus onset included a minimal and peak value difference of over 200μV or MEP was visually inspected from the background activity. User inputted if trial evoked a response or not to MTAT, which prescribed the next trial stimulus intensity. Based on all the trials MTAT presented an approximation of the AMT and a total of 14 stimuli were used to define AMT [mean 36.4(±3.2)of%SMO]. AMT was rounded to the nearest integer. A torque level of 20%MVC worked as a target level for each AMT trial, which has been shown to give maximal MEPs similar to torque level of 50% without the risk of residual fatigue (Temesi et al. 2014). Subjects were instructed to elevate torque to target level when the timer went zero and computer played a beep tone. System

triggered TMS stimulus automatically when torque started to plateau at the target level. Subject stopped producing force immediately after stimulus. Trials followed in clusters of four separated by 10-s and with inter-trial interval of 6-s.

Recruitment curve measurement. An intensity range of 80–180% relative to AMT was divided into 11 intensity levels. Four stimuli were given at each intensity level similar to protocol of Kukke et al. (2014). Total of 44 stimuli in randomised order were given during activation of 20%MVC. MEP relative to Mmax was recorded to obtain recruitment curve. Trials were clustered in sets of four separated by 15-s and with inter-trial interval of 8-s. Recruitment curve protocol was performed before the first fatigue block (Block1) and after second fatigue block (Block2), but not in between blocks. Mmax for normalisation in the POST2 recruitment curve measurement was defined at rest roughly 20-s after the last PVAL stimulus with a 1.3 times the previously used DS intensity.

CVAL intensity measurement. TMS stimulator intensity was defined for CVAL measurements. Target torque level was set to 50%MVC. Subject elevated torque to target level and TMS was triggered automatically at the plateau. An inter-trial interval of 10-s was used. Two stimuli were given at each intensity level. Stimulator output intensity was increased in five percent increments from 50% of SMO until SOL twitch started to decline. Lowest intensity [mean 76.2(±4.6)of%SMO] that evoked maximal twitch was selected for CVAL measurements.

CVAL measurement. CVAL measurement started with a TMS superimposed twitch (SIT) during MVC followed by a subsequent twitch at rest with electric stimulator. α-motoneurons were not maximally recruited, if SIT elicited an increase in torque (Todd et al. 2016). Then TMS SITs were given at torque levels approximately 82.5, 75, 62.5 and 50%MVC (first trial of each VAL measurement). Torque level at the onset of the stimulus was divided by the preceding MVC torque for the corresponding real relative torque level. There was a 18-s rest between all VAL trials. Both MVCs were followed an electric stimulus 2–3-s after at rest. The last trial of each fatigue block was used also as a first TMS SIT for subsequent VAL measurement. Torque plateau was checked 6-s after the initial submaximal torque onset and TMS was triggered accordingly. Subjects were verbally encouraged during MVCs and informed to produce maximal torque while trying to keep head still. There was a 5-min rest after VAL measurement before fatigue Block2. Subjects could stand up during the break.

6.3.4. Percutaneous electrical posterior tibial nerve stimulation

Electrical stimulation was applied with a constant-current stimulator (DS7AH; Digitimer, Cambridge, UK) using a single rectangular pulse (1-ms). Tibial nerve was stimulated on the popliteal fossa with a circular cathode with area of 0.77cm^2 (Unilect 4535M, Ag/AgCl; Uno-medical, Redditch, UK). An oval-shaped anode with a size of 5.08x10.16cm (V-trodes; Mettler Electronics, Anaheim, CA) was placed at middle of the patella tendon. Three to five different cathode locations were stimulated with an intensity that evoked visually inspected SOL M-wave. Location with a biggest M-wave amplitude and minimal TA M-wave was selected as the stimulation site and attached a self-adhesive Ambu WhiteSensor WS-00-S Ag/AgCl ECG electrode with a diameter of 36x40mm (Ambu A/S, Ballerup, Denmark).

Compound muscle action potential measurements. Electric constant current stimulator intensity was increased in steps of 10mA until M-wave started to plateau, the intensity step was lowered to 2–5mA until no increase in M-wave amplitude was seen or it started to decline. The first intensity that elicited the Mmax was multiplied by a factor of 1.3 for supramaximal intensity which was used afterwards for all the electric stimuli in the current session (Rozand et al. 2015) excluding reference Mmax used for POST2 recruitment curve protocol. Mmax was defined to be the maximal peak-to-peak amplitude of the M-wave. Interstimulus interval was at minimum 8–10-s.

Peripheral VAL measurement. After the TMS SITs another MVC with SIT induced by electric stimulator was done followed by electric stimulus at rest to determine PVAL. Potentiated twitch applied 2–5-s after SIT is used to account for the state of muscle during contraction (Todd et al. 2016).

6.3.5. Rating of perceived exertion

Subjects RPE was surveyed digitally (iPad Pro + Apple pencil, Apple) on a 10cm horizontal visual analog scale (VAS) from 0–10 before, in between and after the fatigue blocks. Subject was instructed to draw a vertical line corresponding to the current state of physical and mental exertion. Numbness or any physical or mental pain was also encouraged to be taken into

account in the self subjective measure. RPE value could receive values over 10 if subject had drawn line outside of the box, but not values below zero.

6.3.6. Electroencephalography

EEG data was measured with a 21 channel BrainCap EEG system (Brain Products GmbH, Germany) which consisted of an amplifier (32+8 channels QuickAmp, Twente Medical Systems International B.V., Netherlands) and a recording software (BrainVision Recorder Professional V. 1.20.0801, Brain Products GmbH, Germany). Additionally contralateral mastoid, SOL, TA electrodes and a separate torque trigger cable were connected to the EEG amplifier. When ankle dynamometer torque elevated above 25Nm a trigger signal was delivered to the amplifier. Amplifier low-pass cutoff frequency was set to default at 280Hz. Measuring tape was used to locate half of the distances from nasion to inion and pre-auricular points. Crossing of the half point marked the location for the vertex, which was marked with a marker pen. Reference electrode was attached on the forehead. Skin was wiped with disinfectant before attaching self-adhesive electrodes for reference and mastoid Ambu BlueSensor N-00-S Ag/AgCl ECG electrodes with a diameter of 33x22mm (Ambu A/S, Ballerup, Denmark). EEG cap was firmly taped on the forehead to avoid any shifting during head movements. A wooden stick was used to push hairs aside under each electrode and the skin was gently scraped. Electrode holes were filled with EEG gel using a blunt syringe. Wooden stick was twisted and rotated in each electrode hole and gel was filled until impedance lowered under 5kΩ for at least for nine most central electrodes.

6.4. Data analysis

Spike2 scripting language (v4.11; Cambridge Electronic Design Ltd, Cambridge, UK) and Python programming language were used to process torque, EMG and EEG signals. Spike was used to calculate every protocols trials torques and responses that were outputted to external text files. Files were converted into Pandas dataframes for statistical analysis, which was done with open-source scientific computing Python library SciPy (Virtanen et al. 2020). Also Python packages Seaborn, Matplotlib and Statannot were used for plotting. VisionRecorder files were loaded into MNE-Python (Gramfort et al. 2013) raw files for analysis.

6.4.1. Torque

Torque was defined as the peak torque in a time window, which started from torque rising above 50Nm and ended when falling below respectively. For the trials where stimulus response EMG onset could be detected torque was defined as the mean torque of 100-ms time window preceding the EMG onset or otherwise the trigger onset. Torque onset was defined as the mean torque of 50-ms time window elevating above 25Nm. Torque onset check was refreshed every five milliseconds.

PRE torque was defined as the maximum torque of the MVC protocol. Fatigue blocks first and last trials torques where also used. Some of the subjects failed the first or last trial of the fatigue blocks by elevating torque too early and misguiding the measurement system for a completed trial. In these cases trials were adjusted to correspond successful first and last trial. Fatigue trials torque below 100Nm and control trials torque below 15Nm were dropped.

6.4.2. Electromyography

EMG of the VisionRecorder was bandpass filtered at 10–280Hz using hamming finite impulse response (FIR) window and firwin filter design. In one of the subjects sessions EMG cable that was connected to EEG amplifier was broken and EMG had to be converted from Spike recordings. EMG was split into epochs preceding torque onset of the fatigue trials by 2.5-s.

For the EMG onset detection EMG was high-pass filtered at 20Hz and notch filtered at 50Hz. EMG onset definition was adjusted according to EMG noise and to the type of the recording system. Baseline was set at range -2.5–(-2.0)-s relative to torque onset. Upper and lower thresholds for the EMG onset were set relative to plus/minus three times the baseline SD. In the default setting EMG onset was marked as the minimum of three subsequent peaks or troughs above or below threshold clustered together within 20-ms segment. Rolling SD of 3-ms from -1.5-s to torque onset was inspected for peaks to catch more uniform increasing activity. Starting times for the EMG onset search ranges were calculated by shifting SD peak times by two times the peak/trough cluster length. Thresholds, peak/trough density, peak/trough cluster length and onset rolling window length were configured manually for trials with erroneous EMG onsets. Each trial EMG onset detection settings were saved to disk. Subject 3 run 2

EMG onsets used unique onset definition (voltage under or above ±3 x baseline[-2.5:-1-s to torque onset] SD) that was run in Spike. Trials which EMG onset could not be defined were dropped from the later analysis.

6.4.3. Responses

A pre EMG onset torque baseline of 20-ms to EMG onset was used as the reference torque for twitch response. A pre-stimulus baseline of 100-ms to stimulus onset was used to define lower and upper thresholds of three times the baseline SD and post-stimulus interval s of 5–25-ms for the M-wave and 25–75-ms for the MEP were used to search EMG onset. Pre EMG onset torque baseline was subtracted from the maximum torque during interval of 500-ms from EMG onset to define twitch torque.

CVAL. Twitch amplitude of each TMS SITs relative to Mmax twitch was calculated. MVC SIT was divided by extrapolated resting twitch and this was subtracted from one and multiplied by 100 to define CVAL. Linear regression line was fitted on the TMS SITs to extrapolate resting twitch as described by Dekerle et al. (2019a and 2019b). Negative twitches in the trials where torque was declining were set to zero. Sessions missing two or more CVAL measurements were not included in the analysis. One of the subjects CVAL was calculated by only using three SITs. Negative twitches were converted to zero.

PVAL. Subjects sessions missing two or more PVAL measurements were left out. PVAL was calculated by normalising SIT during MVC to the following resting twitch, and subtracting it from one and then multiplying by 100% (Todd et al. 2016).

Recruitment curve. MEPs and stimulus intensities were normalised as previously described. Mean peak-to-peak MEP at each intensity was calculated and grand average across subjects was taken to create recruitment curve. The total area under the recruitment curve (AURC) was integrated using the composite trapezoidal rule (Carson et al. 2013). Also a sigmoid function was fitted into the original 44 MEPs using non-linear least square method:

$$MEP = EMG_{base} + \frac{MEP_{sat}}{1 + e^{\frac{s_{50} - s}{k}}} \quad (1)$$

where EMG_{base} is the EMG activity without identifiable MEPs at low intensities, MEP_{sat} is the plateau of the response amplitude at high intensities, s_{50} is the stimulation intensity evoking response half-way between EMG_{base} and MEP_{sat}, and k is the derivate of the response-intensity-curve from the point at s_{50} to a point where MEP at s_{50} has increased 73% (Kukke et al. 2014).

6.4.4. Cortical silent period

CVAL trials raw EMG -200 to +800ms relative to stimulus onset was exported into external text files and then converted into Pandas dataframes for cortical SP analysis. EMG was butterworth bandpass filtered at 60–450Hz to remove strong DC drifts after the stimuli. Cortical SP attenuation was searched 30ms after MEP latter trough or peak. A 200ms search window was divided into 30ms bins overlapping by 28ms. SD of each bin was calculated and bins with a local peak of minimum of 50 bins and SD over 20μV were selected. Criterion for local count of bins was reduced by 10 if no matched peaks were found. Four bins around each peak and peak bin included were inspected for cortical SP attenuation starting from the earliest bin. Baseline included all of the preceding bins and the selected bin. Upper and lower thresholds for cortical SP attenuation were defined as the mean±3SD of baseline, respectively. The first sample of the bin outside thresholds that was preceded by a train of five consecutive samples (segment of 1-ms with a 5kHz sampling frequency) inside thresholds was defined as the cortical SP attenuation. In five trials attenuation parameters were adjusted by lowering the thresholds to 2.5SDs and lengthening the segment inside thresholds before cortical SP attenuation (2–6-ms). Stimulus onset was subtracted from the cortical SP attenuation for cortical SP. Trials which cortical SP could not be defined or were duplicates because of double triggering were dropped. One subject was left out for missing both PRE and POST1 measurements in both sessions. Finally grand average of subjects was taken.

6.4.5. Rating of perceived exertion

VASs were converted into images and analysed with OpenCV image shape detection library. Vertical lines middle position relative to scale was converted into a number between 0–10 with algorithm and in unclear cases manually. Lines outside VAS were set manually and received values either zero or over 10. VASs with no lines were dropped. Subjects missing

two or more measurements in any of the sessions were left out. Finally grand average of subjects RPE was taken.

6.4.6. Readiness potential

EEG montage was set to standard 10-20. EEG was FIR bandpass filtered at 0.01–35Hz using hamming window and firwin filter design. Raw data was sliced into epochs 2.5-s pre EMG onsets. Mean of all the electrodes was used as a reference. Trials without EMG onset and manually inspected bad trials were dropped before Autoreject algorithm (Jas et al. 2017).

EEG preprocessing with Autoreject. Flowchart of the preprocessing pipeline leading to final clean epochs is shown in the figure 9. Noisy and flat channels were interpolated in three separate stages: 1) flat channels before autoreject, 2) noisy channels by second run of autoreject, and 3) the noisiest channel from the nine vertex channels that met epoch occurrence criteria. Epochs were rejected also in three different stages: 1) by first run of autoreject, 2) by second run of autoreject, and 3) by ±200μV peak-to-peak amplitude threshold criteria for the vertex channels. Flat channels containing peak-to-peak under 0.1μV within epochs were interpolated using MNE spherical spline method and epochs were baseline corrected in the interval of -2.5–(-2.0)-s relative to EMG onset. Autoreject fit was run using fixed random state and bayesian optimization. Autoreject was run with the following parameters: the maximum number of interpolated EEG channels ρ was tried in the order of 1, 4 and 9 and the maximum number of bad sensors κ as a fraction of total number of sensors (consensus) in a non-rejected trial was set to default with 10% steps from zero to 100%. (Jas et al. 2017.) Autoreject was run twice. The purpose of the first run was to detect bad epochs before independent component analysis (ICA) fit, but without any transformation. This enabled ICA to focus on clean epochs without excessive interpolation of channels. Second run of autoreject then transformed ICA corrected epochs which were also baseline corrected. After the second run of autoreject, the nine most central channels (F3, Fz, F4, C3, Cz, C4, P3, Pz, P4) were selected as vertex channels. From these channels the most frequent (minimum occurrence of five epochs) channel containing peak-to-peak amplitude of over ±200μV was interpolated. Epochs containing at least one vertex channel with a peak-to-peak amplitude of over ±200μV were rejected. From the total of 1140 epochs 358 epochs were rejected by second run of autoreject and 83 by ±200μV vertex

channel threshold totalling 441 dropped epochs. For the second run of the autoreject mean consensus was 0.47 and mean interpolated channels per good epoch was 2.34 and from the vertex channels 0.34 was interpolated per good epoch (table 3).

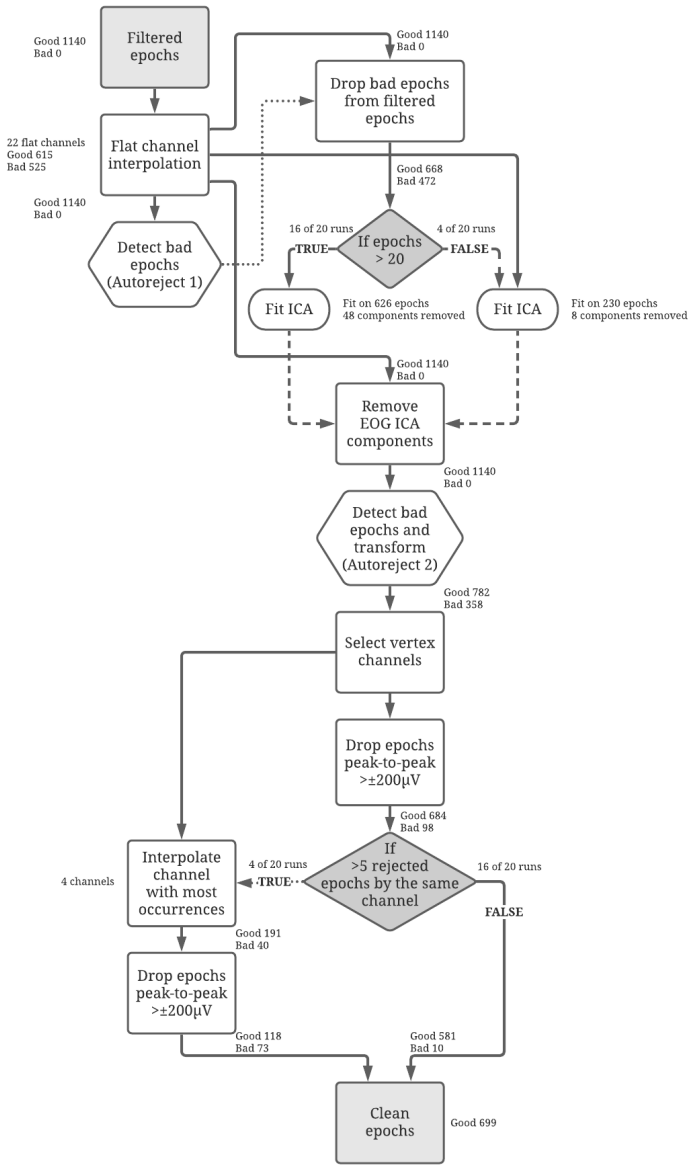

FIGURE 9. Preprocessing pipeline from filtered epochs to clean epochs. Solid lines describe processed epochs as an input to next processes. Dotted lines describe calculation input to be used in the following process for either dropping epochs or channel interpolation. Dashed line describes fit input to be used in removing ICA components. Diamond shapes describe logical operation for the selection of the following process. Hexagon shapes describe autoreject processes. Good and bad epoch counts are shown after each process. EOG=electrooculography, ICA=Independent component analysis.

TABLE 3. Interpolated channels and their proportions in 782 good epochs transformed by second run of autoreject.

channel	n	%
Fp1	213	27.2
Fp2	135	17.3
F3	121	15.5
F4	22	2.8
C3	27	3.5
C4	50	6.4
P3	21	2.7
P4	54	6.9
O1	168	21.5
O2	43	5.5
F7	63	8.1
F8	118	15.1
T3	63	8.1
T4	147	18.8
T5	85	10.9
T6	112	14.3
Fz	65	8.3
Cz	91	11.6
Fpz	112	14.3
Pz	22	2.8
Oz	105	13.4

EEG independent component analysis. Frontal channels (Fpz, Fp1 and Fp2) were set as electrooculography channels and bandpass filtered at 1Hz. Then correlation between electrooculography channels and ICA components were calculated. Top three most positively or negatively correlated ICA components with a minimum correlation scores of 0.3 were removed. Interpolated flat channel count plus one for mean reference were subtracted from the total number of EEG channels to calculate number of dimensions for the ICA fit (MNE-python, 2020).

Readiness potential slope categorization. Epochs were converted into trials dataframe for the RP slope categorisation. Trials were divided into RP components BL1, BL2, RP1, RP2 and NS', with time-windows of -2.5–(-2.0)-s, -2.0–(-1.5)-s, -1.5–(-1)-s, -1–(-0.5)-s and -0.5–0-s relative to EMG onset, respectively (figure 10). For each trial mean of the components time-window was calculated. A linear first order regression fit was applied into the grand medians of the means of readiness potential components of the nine vertex channels. RP was categorised as positive if the slope of the fit was even or above zero and otherwise set to negative.

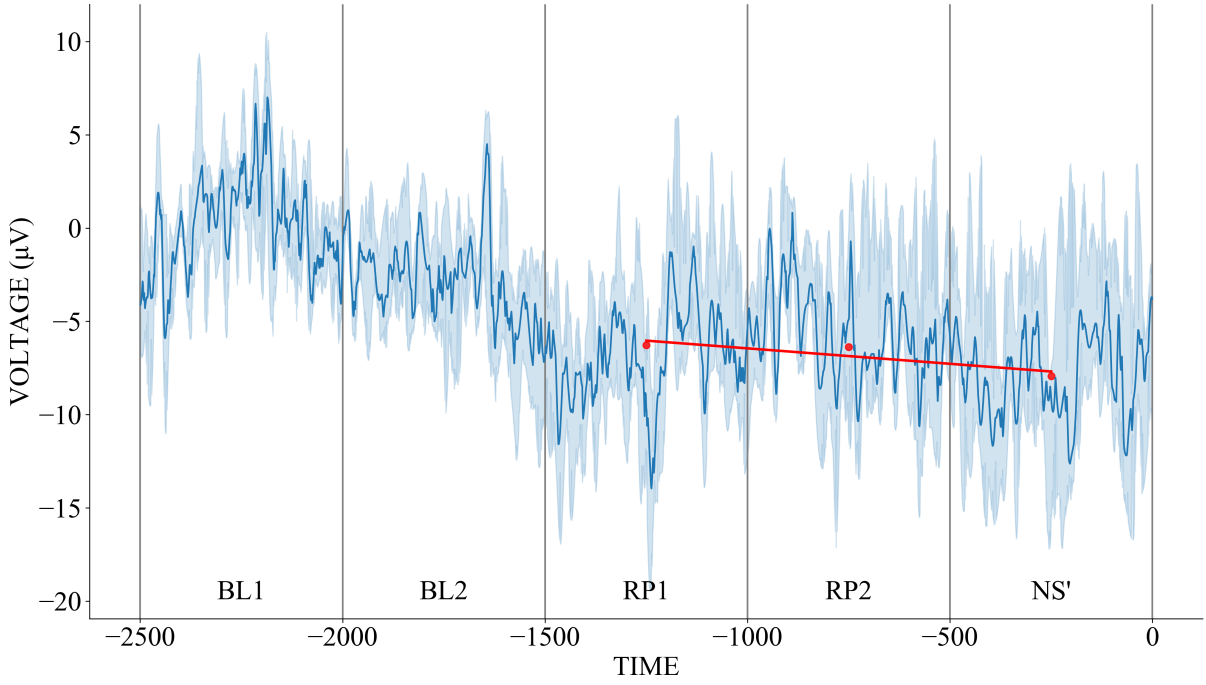

FIGURE 10. Single trial mean vertex channels readiness potential components with a fit into medians of RP1, RP2 and NS'. Grand median signal of the vertex channels is shown as a blue trace with a 95% confidence interval (in actual calculations components means were first calculated for each vertex channel separately, and then the grand medians of those means were used for fitting). Medians of the means of components RP1, RP2 and NS' of the vertex channels are shown as red dots. Linear first order regression fit of medians is shown as a red line. Trial was categorised as negative by the negative slope of the fit. BL=baseline, RP=readiness potential, NS'=negative slope.

6.5. Statistical analysis

Measurements were compared within and between control and fatigue sessions. All the statistical tests used non-parametric Kruskall-Wallis H-test of equality of medians with alpha level set to 0.05. Change in RP parameters amplitude of RP1, RP2 and NS' and slope occurrence difference from Block1 to Block2 were tested with Pearson correlation with change in AURC, CVAL, PVAL, cortical SP and torque from PRE to POST2. Correlation test alpha level was set to 0.05. Tests were run with Python.

Torque. The grand average of torque was compared before fatigue Block1, at the beginning and end of every fatigue block.

VAL. The grand average of the cortical and PVAL were compared before fatigue Block1 and at the end of fatigue Blocks1–2. Subject 2 was dropped from the analysis due to very low cortical twitches compared to group. Subject 5 fatigue session CVAL measurements were dropped because of unusually low PRE responses. Subject 7 fatigue session CVAL measurements were dropped because of missing measurements. Subject 9 all VAL measurements were dropped because of missing measurements.

Recruitment curve. The grand average of the total AURC and sigmoid fit parameters EMG_{base}, EMG_{sat}, s_{50} and k were compared before fatigue Block1 and after fatigue Block2.

Cortical SP. The grand average of the cortical SP measured during CVAL protocol was compared before fatigue Block1 and after fatigue Blocks1–2. Subject 9 was rejected for missing measurements.

Rating of perceived exertion. The grand average of RPE was compared before fatigue Block1 and after fatigue Blocks1–2. Subject 7 control session was rejected for missing measurements.

Readiness potential. RP components BL1, BL2, RP1, RP2 and NS' were calculated in each trial as time-window means. Then subject grand median of trial components were grouped into early (Block1, 30 trials) and late (Block2, 30 trials) blocks, control and fatigue sessions and positive and negative RPs. Grand median components were compared within and between sessions and blocks. Positive and negative RP slope occurrences were compared between blocks within and between sessions. Subjects sessions containing at least one block under 10 trials were dropped making 144 dropped trials. 8 subjects were qualified for control session and 5 for fatigue session making the final total trial count 555 (control=353 and fatigue=202).

7. RESULTS

7.1. Fatigue measures

7.1.1. Torque

Torque decreased significantly during fatigue session from PRE 291±41Nm to last trial of Block1 211±37Nm and Block2 200±36Nm (1-last: H=9.6, p=0.002; 2-last: H=11.1, p=0.001). There was a similar non-significant trend during the control session (1-last: H=3.8, p=0.050; 2-last: H=2.9, p=0.086). (figure 11.)

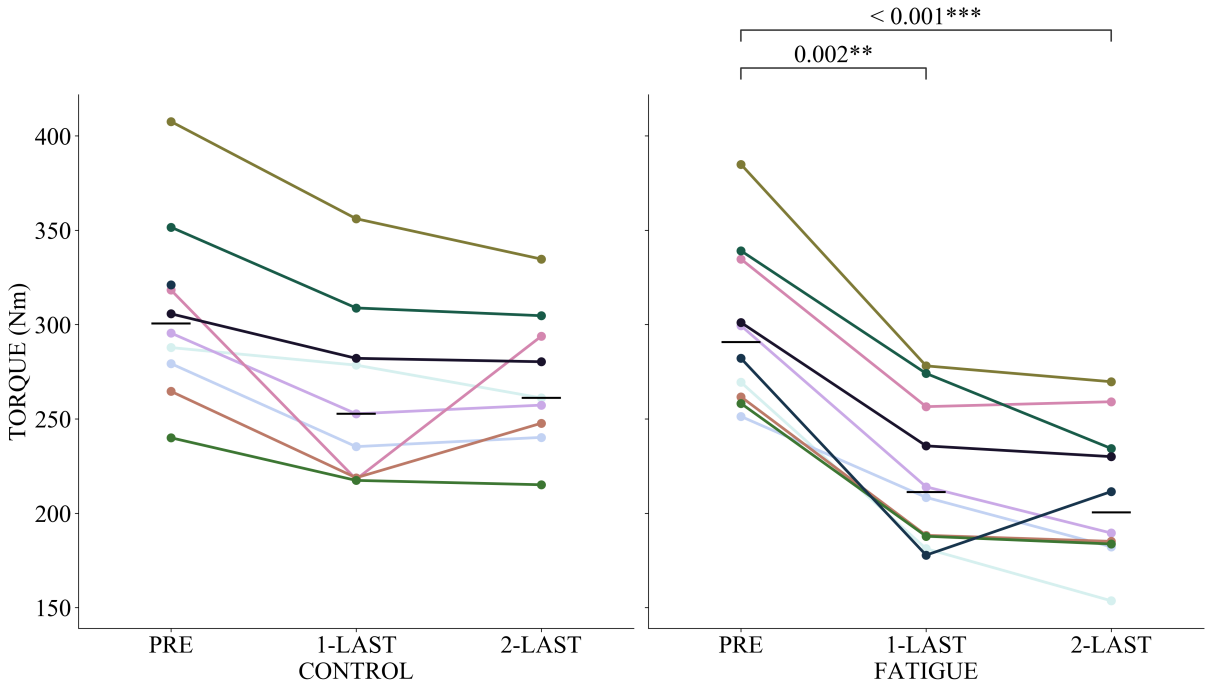

FIGURE 11. Isometric ankle plantarflexor MVC torque before control/fatigue protocol and at the end of Block1–2 with group medians. Subjects are separated by hue. Kruskall-Wallis H-test of equality of medians with alpha level set to 0.05. Notation for P-value: **:p<=0.01 and ***:p<=0.001.

7.1.2. Peripheral VAL

PVAL decreased significantly after fatiguing protocol from PRE 99±2% to POST1 89±5% (H=7.26; p=0.0071) and from PRE to POST2 93±5% (H=8.75; p=0.0031), but not from POST1 to POST2 (figure 12).

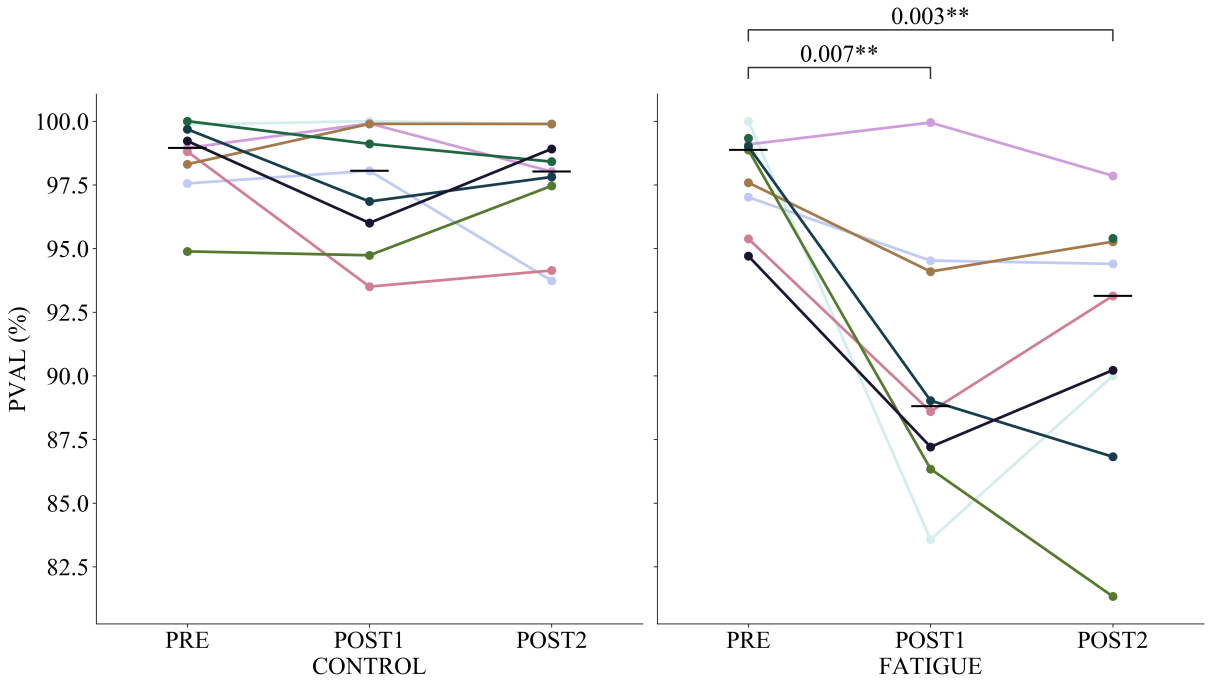

FIGURE 12. Peripheral voluntary activation level (PVAL) before control/fatigue protocol, and at the end of Block1–2 with group medians. Subjects are separated by hue. Kruskall-Wallis H-test of equality of medians with alpha level set to 0.05. Notation for P-value: **:p<=0.01.

7.1.3. Rating of perceived exertion

During fatigue RPE increased significantly from PRE 1.2±2.3 to POST1 6.7±2.2 (H=9.1, p=0.003) and POST2 8.4±2.0 (H=11.6, p=0.001). There was a similar non-significant trend during control session. (figure 13.)

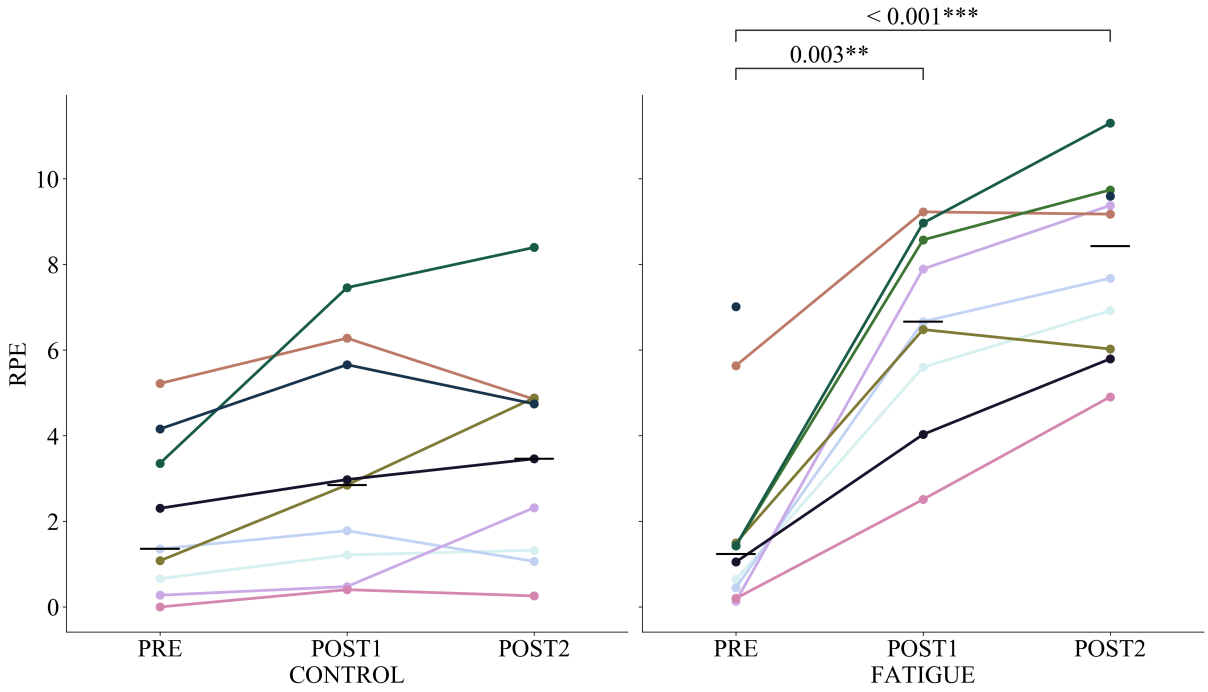

FIGURE 13. Rating of perceived exertion (RPE) before control/fatigue protocol, and at the end of Block1–2 with group medians. Subjects are separated by hue. Kruskall-Wallis H-test of equality of medians with alpha level set to 0.05. Notation for P-value: **:p<=0.01, and ***:p<=0.001

7.2. EEG measures

7.2.1. Readiness potential

RPs were grouped by block, session and by the slope of the linear fit on the median of the vertex channels at RP1, RP2 and NS'. The negative grand median Cz RP across subjects median RPs looks similar in all groups. Confidence intervals are visibly higher in groups with smaller sample sizes as seen during fatigue. (figure 14.)

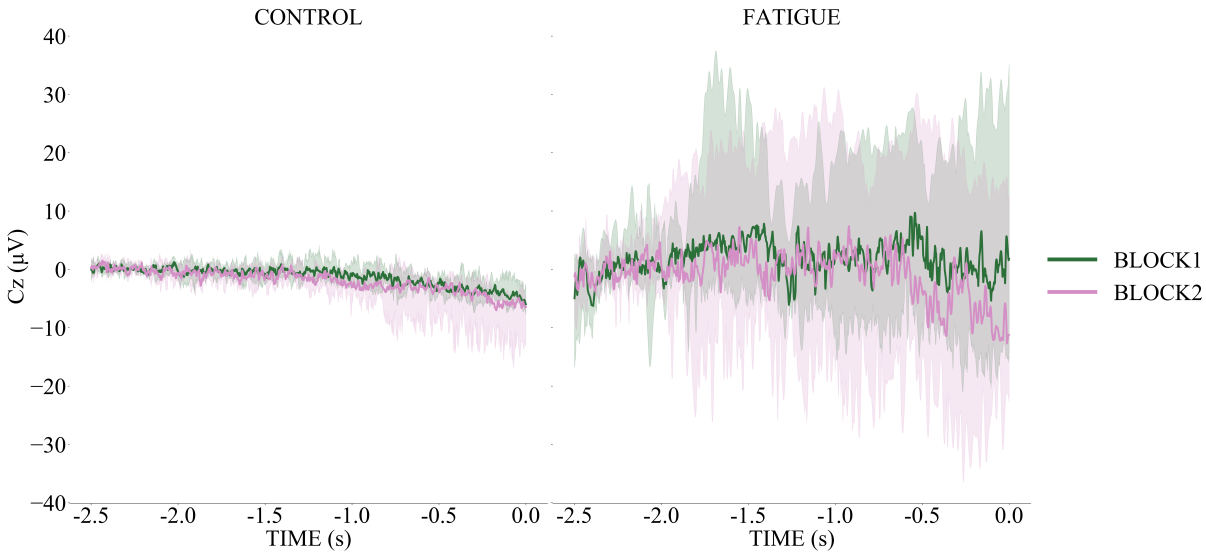

FIGURE 14. Grand median Cz negative slope RP of subject median RP grouped by block with 95% confidence intervals. Block1 includes the first 30 trials and Block2 the last 30 trials. Subject and trial occurrences: control (n=8): Block1 (trials=120), Block2 (trials=103), fatigue (n=5): Block1 (trials=38), and Block2 (trials=30).

The positive grand median Cz RP across subjects median RPs increased during fatigue. Increase in amplitude was more profound near EMG onset. (figure 15.)

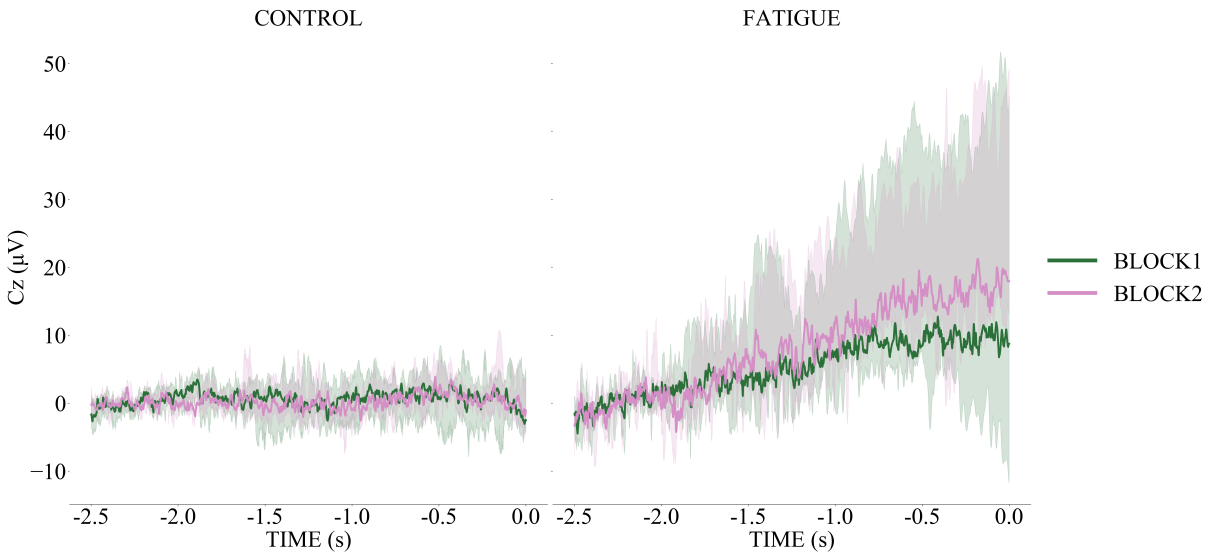

FIGURE 15. Grand median Cz positive slope RP of subject median RP grouped by block and session with 95% confidence intervals. Block1 includes the first 30 trials and Block2 the last 30 trials. Subject and trial occurrences: control (n=8): Block1 (trials=71), Block2 (trials=59), fatigue (n=5): Block1 (trials=77), and Block2 (trials=57).

RP was divided into time components for comparison: BL1, BL2, RP1, RP2 and NS', with time-windows of -2.5–(-2.0)-s, -2.0–(-1.5)-s, -1.5–(-1)-s, -1–(-0.5)-s and -0.5–0-s relative to EMG onset. During control positive RP amplitude did not differ significantly from the baseline in Block1–2 (table 4).

TABLE 4. Positive slope RP components during control (n=8).

component	µV	BL2	RP1	RP2	NS'
BL1	Block1 0.0±0.0	1.0±5.6	-0.5±7.7	0.8±9.3	1.0±15.2
BL1	Block2 0.0±0.0	0.2±1.2	0.4±7.3	0.2±9.1	0.2±10.1

During control negative RP amplitude decreased significantly from the baseline BL1 with NS' in Block1 and RP2 and NS' in Block2 (table 5).

TABLE 5. Negative slope RP components during control (n=8).

component	µV	BL2	RP1	RP2	NS'
	Block1	-0.0±1.5#	-0.4±3.1	-1.0±3.4	-4.1±4.2#
BL1	0.0±0.0				H=6.4, p=0.01172
	Block2	-0.9±3.4§	-1.2±5.5	-3.2±9.7	-4.4±9.4§
BL1	0.0±0.0			H=6.4, p=0.01172	H=11.3, p=0.00078

#: H=5.3, p=0.02086; §: H=5.8, p=0.01571

During control no significant time effect was seen within components in the positive and negative RPs (figure 16).

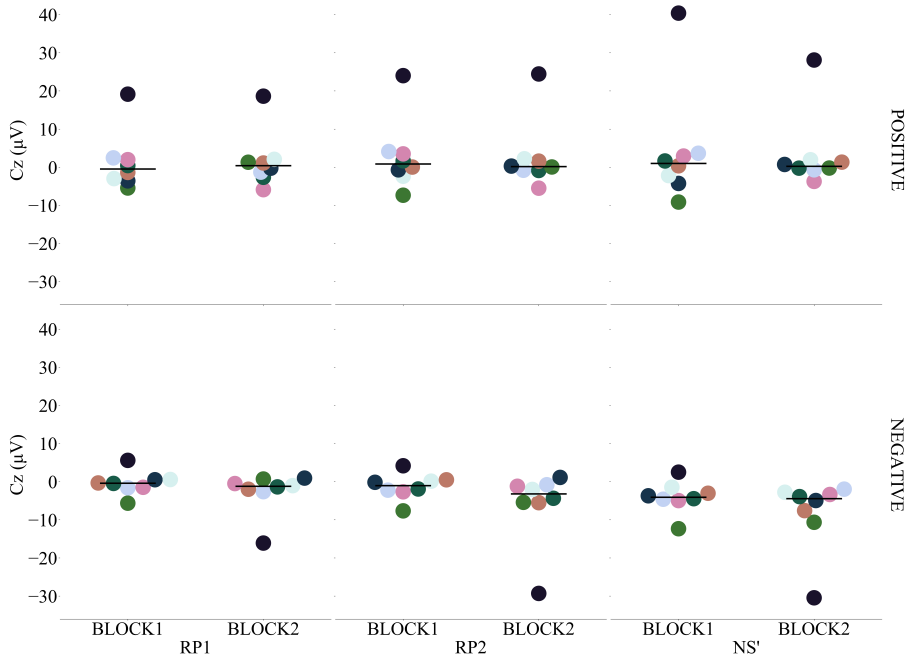

FIGURE 16. Control Cz RP components RP1, RP2 and NS' grouped by block and slope with group medians. Subjects (n=8) are separated by hue. Block1=first 30 trials and Block2=last 30 trials. Positive RP components are shown in the upper row and negative in the lower row.

During fatigue positive slope RP components amplitude increased significantly from the baseline BL1 with RP1, RP2 in Block1 and BL2, RP1, RP2 and NS' in Block2 (table 6).

TABLE 6. Positive slope RP components during fatigue (n=5).

component	µV	BL2	RP1	RP2	NS'
	Block1	2.5±4.0#	4.8±6.6§	8.0±12.4#§	8.9±15.5
BL1	0.0±0.0		H=6.8, p=0.00902	H=6.8, p=0.00902	
	Block2	1.8±1.6^♦	10.5±6.4	12.3±5.6^	15.8±13.6♦
BL1	0.0±0.0	H=6.8, p=0.00902	H=6.8, p=0.00902	H=6.8, p=0.00902	H=6.8, p=0.00902

#: H=3.9, p=0.0472; §: H=3.9, p=0.0472; ^: H=6.8, p=0.00902; H=6.8, p=0.00902; ♦: H=6.8, p=0.00902

During fatigue negative RP amplitude did not differ significantly from the baseline BL1 in Block1–2 (table 7).

TABLE 7. Negative slope RP components during fatigue (n=5).

component	µV	BL2	RP1	RP2	NS’
BL1	Block1 0.0±0.0	3.7±8.2	2.5±6.5	3.9±11.3	-1.4±14.8
BL1	Block2 0.0±0.0	-2.0±11.2	2.0±13.8	0.8±14.3	-7.4±17.5

During fatigue no significant time effect was seen within components in the positive and negative RPs (figure 17).

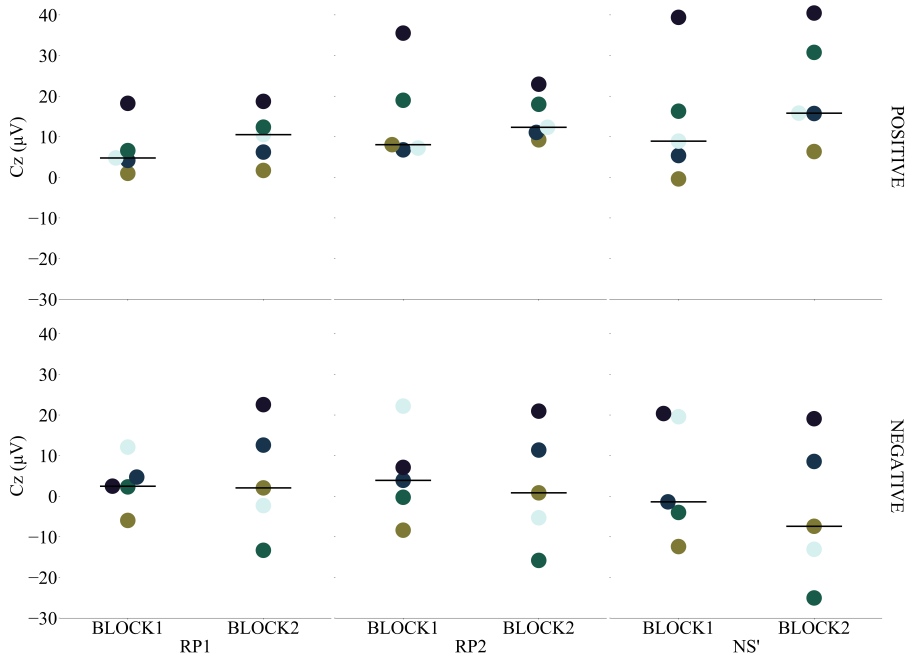

FIGURE 17. Fatigue Cz RP components RP1, RP2 and NS’ grouped by block and slope with group medians. Block1: first 30 trials and Block2: last 30 trials. Subjects (n=5) are separated by hue. Positive RP components are shown in the upper row and negative in the lower row.

There was a non-significant effect within block in the occurrences of positive and negative RPs (figure 18). Fatigue condition consisted of significantly more positive RP trials measured as a difference between positive and negative trials (Block1: 5.0±12.9, Block2: 2.0±6.2) than control condition ([Block1: -5.5±6.2, H=3.9, p=0.0472], [Block2: -6.0±3.8, H=8.2, p=0.0041]). Significant slope occurrence dependence to control/fatigue condition was also shown during the first five trials: control -3.0±1.7 and fatigue 2.0±3.0 (H=4.1, p=0.0417).

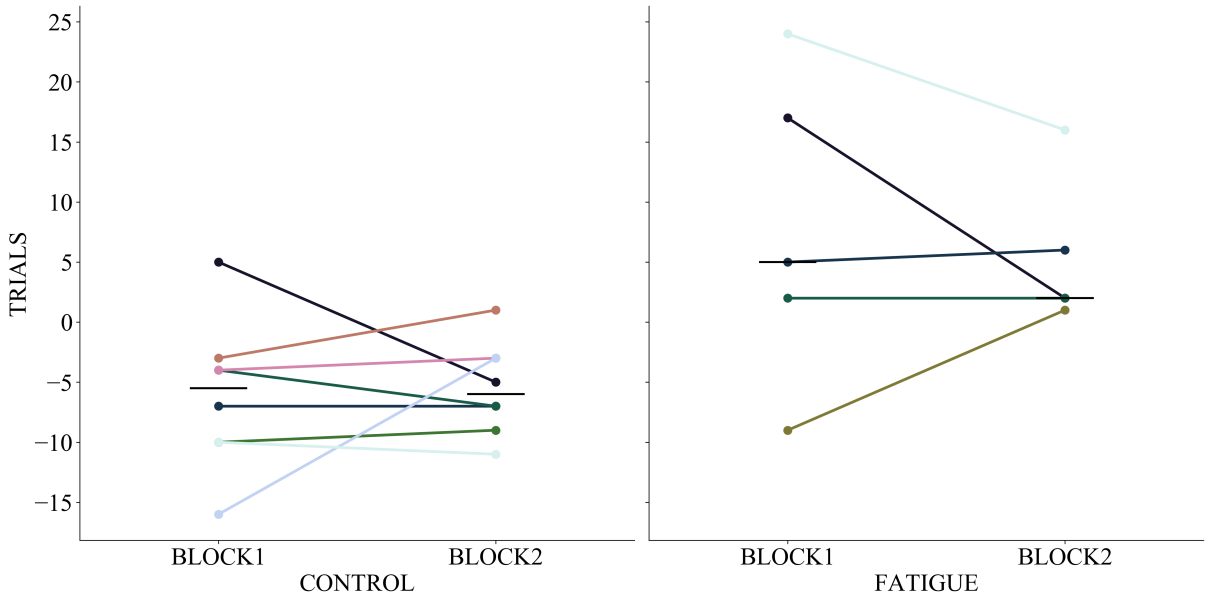

FIGURE 18. Control (n=8) and fatigue (n=5) difference of positive and negative RP occurrences grouped by block. Lines correspond the group medians. Subjects are separated by hue.

During fatigue there was a significant negative correlation (r=-0.97, p=0.0063, n=5) between change in positive RP2 amplitude from Block1 to Block2 and decrease in torque from PRE to POST2 (figure 19). No significant or visually valid correlation was found between RP components RP1, RP2 and NS' amplitude change from Block1 to Block2 and change in AURC, CVAL, PVAL and cortical SP from PRE to POST2. Change in occurrences of RP slopes from Block1 to Block2 did not correlate significantly with AURC, CVAL, PVAL, cortical SP and torque from PRE to POST2.

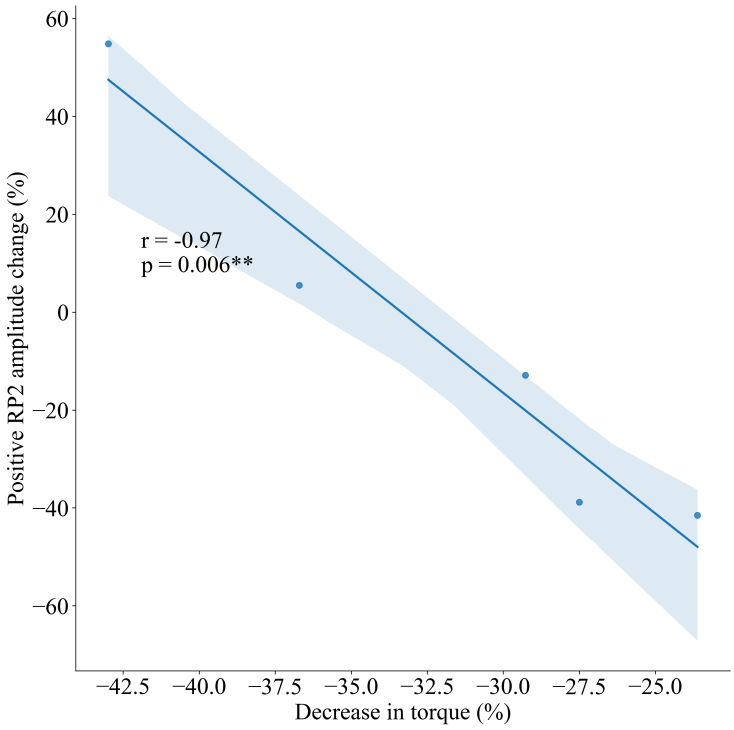

FIGURE 19. Pearson linear regression fit with 95% confidence interval between change in positive RP2 amplitude from Block1 to Block2 and decrease in torque from PRE to POST2 during fatigue. Pearson correlation test with alpha level set to 0.05. Notation for P-value: **:p<=0.01

7.3. TMS measures

7.3.1. Cortical VAL

CVAL decreased significantly after fatiguing protocol from PRE 91±5% to POST2 80±14% (H=5.0, p=0.025) (figure 20).

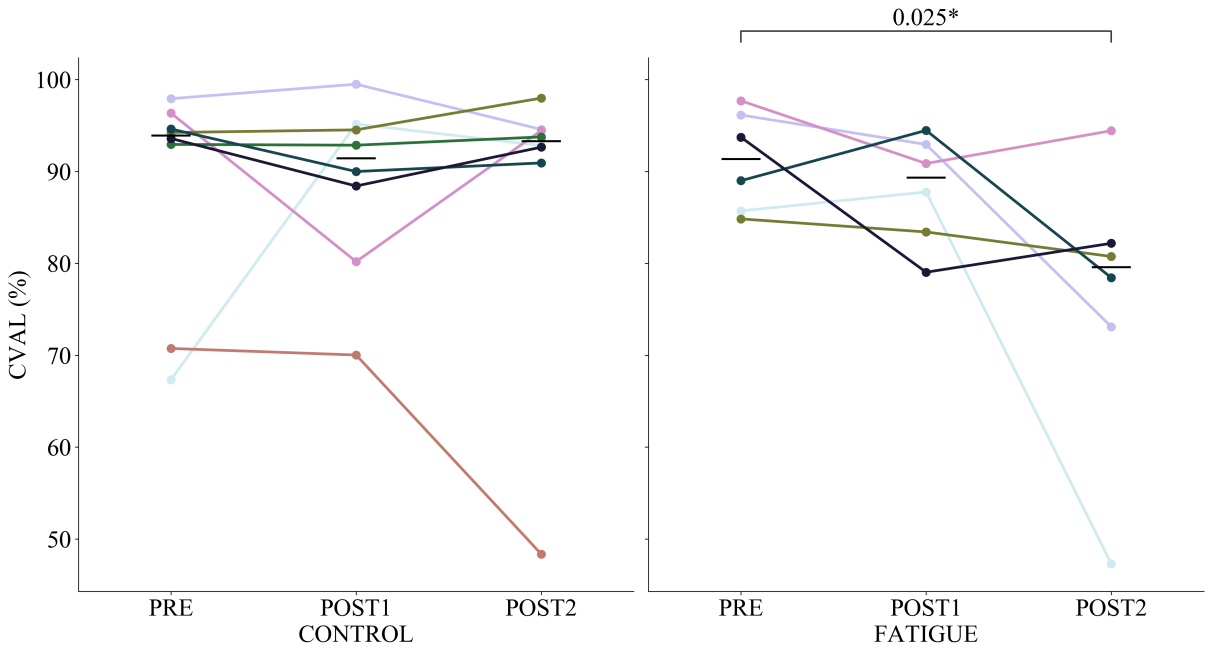

FIGURE 20. Cortical voluntary activation level (CVAL) before control/fatigue protocol, and at the end of Block1–2 with group medians. Subjects are separated by hue. Kruskall-Wallis H-test of equality of medians with alpha level set to 0.05. Notation for P-value: *:p<=0.05.

7.3.2. Recruitment curve

During both sessions there was a trend of increased CSE from PRE to POST2 (figure 21).

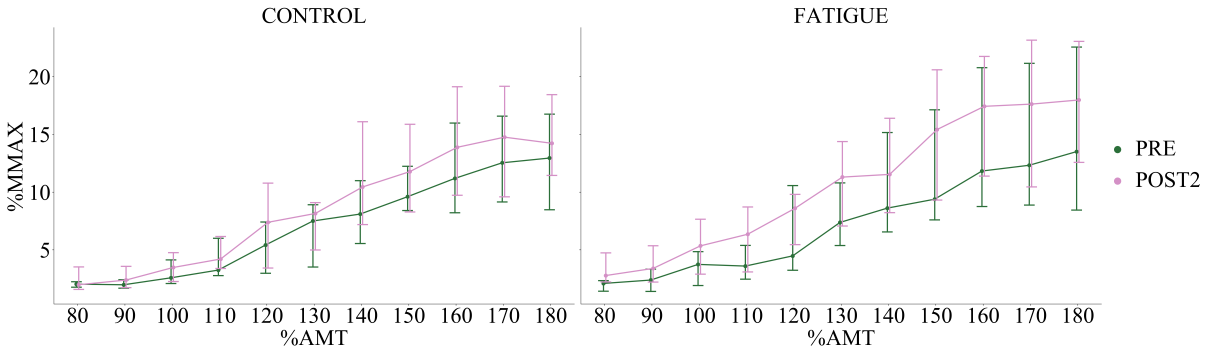

FIGURE 21. Grand median recruitment curve normalised to Mmax with 95% confidence intervals using means of four intensity-response pairs at each active motor threshold (AMT) relative intensity level.

Total AURCs were non-significantly changed during both conditions (figure 22).

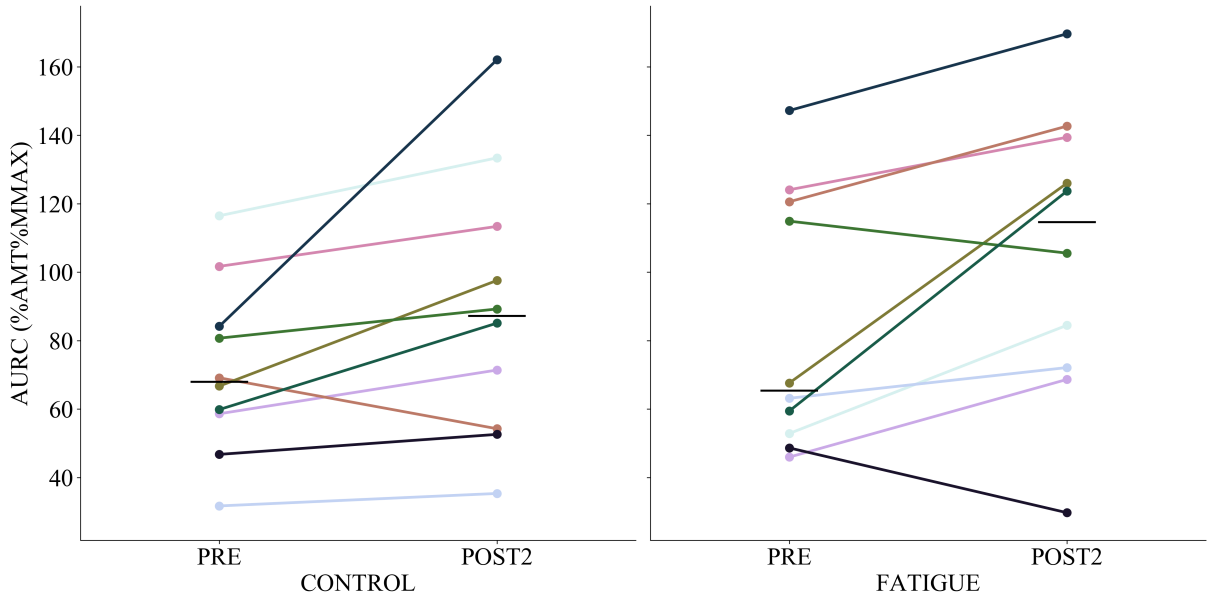

FIGURE 22. Total area under the recruitment curve (AURC) before and after control/fatigue protocol with group medians. Subjects are separated by hue.

7.3.3. Cortical silent period

During fatigue cortical SP decreased significantly from PRE 0.144±0.011-s to POST1 0.132±0.012-s (H=4.3, p=0.038) and POST2 0.134±0.011-s (H=4.0, p=0.047) (figure 23).

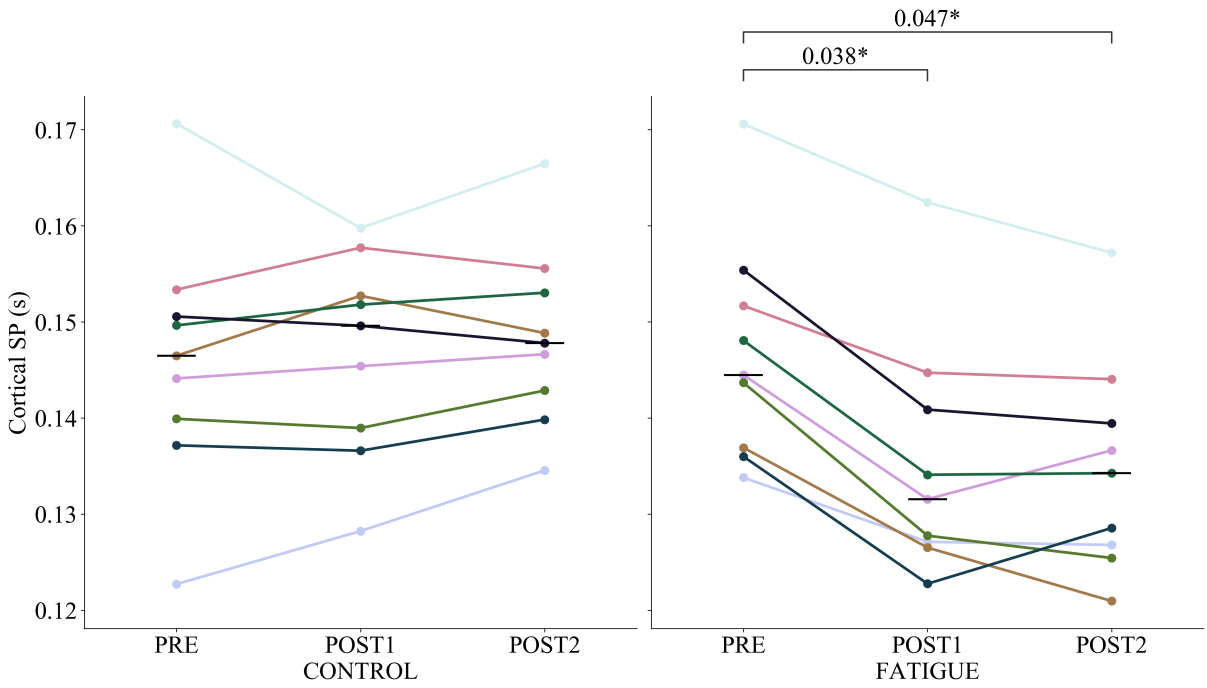

FIGURE 23. Cortical silent period (SP) before control/fatigue protocol, and at the end of Block1–2 with group medians. Subjects are separated by hue. Kruskall-Wallis H-test of equality of medians with alpha level set to 0.05. Notation for P-value *:p<=0.05, **:p<=0.01.

8. DISCUSSION

The present study examined readiness potential preceding isometric contraction of triceps surae muscles and corticospinal excitability in fatigued and control conditions. Focus was on the relationship between readiness potential and degree of fatigue. Main findings showed a decreased torque, CVAL, PVAL, and shortened cortical SP with increasing RPE during fatigue. Readiness potential showed a progressively increasing negative and positive drift starting 1.5-s before EMG onset. Negative readiness potentials amplitude got more negative during control and positive readiness potentials got more positive during fatigue. There was a significantly larger occurrence of positive readiness potentials during fatiguing trials, whereas negative readiness potentials were more frequent during control. This was also apparent in the first five trials of the Block1. No modulating effect of level of fatigue on readiness potential amplitude and occurrence of positive and negative readiness potentials was seen. On the other hand during fatigue, change in positive RP2 amplitude correlated negatively with a decreased torque. Corticospinal excitability showed a non-significant trend of increase after both protocols. Based on the results, probability of movement ignition in lower activity M1 cortex state is higher during fatigue and M1 cortex modulation is stronger closer to EMG onset. This may suggest that corticospinal excitability increases similarly after fatiguing and non-fatiguing intermittent isometric plantarflexor contractions.

8.1. Premotor brain activity

Previously slope-dependent readiness potentials have only been reported across whole task (Jo et al. 2013). While not significant, higher proportion of positive readiness potentials with a trend of increasing positive readiness potential amplitude during fatigue is in line with study of Spring et al. (2016), which showed a less negative non-slope-dependent readiness potential amplitude during fatigue. Higher occurrence of positive readiness potentials might explain reduced non-slope-dependent readiness potential amplitude, which reflects less active state of cortical pre-motoneuronal circuits (Deecke et al. 1976) and corticospinal motoneurons (Chen et al. 1998). In contrast non-slope-dependent readiness potential amplitude has been reported by several studies to increase or show no change during fatigue (table 2).

Both positive and negative readiness potentials measured during control could result from stochastic spontaneous fluctuation in excitability of neural circuits under decision threshold as suggested by Schurger et al. (2012). Some contractions are started during lower excitability if motivation to act is sufficient, meaning that ignition to move is not only dependent on the phase of the fluctuation. Precision required to control low level of force production during control contractions could act as such an external cue that could mask internal cues related to movement ignition.

The negative correlation found between change in amplitude of positive RP2 and decrease in torque during fatigue suggests shift of M1 cortex neuronal circuits to less favourable (positive readiness potential) state as fatigue progresses with more severely fatigued subjects. Smaller decline in torque could be explained by increased M1 cortex excitability seen as reduced amplitude of late positive readiness potential and it could act as a compensatory mechanism for peripheral fatigue. Positive readiness potential amplitude can also result from increased proportion of negative readiness potentials. There could also be individual differences in the initial proportion and/or amplitude of positive readiness potentials during fatigue. Readiness potential was analyzed from the same channel with every subject and it is possible that vertex channels show a non-uniform individual activity pattern. Some support for this view was inspected during readiness potential slope categorization where inter-channel activity was highly variable.

The difference in readiness potential slope occurrences might be related to unconditioned RFD. Higher RFDs has been shown to increase non-slope-dependent readiness potential amplitude (de Morree et al. 2012; Slobounov et al. 2004). Fatigue-related decrease in RFD could result in lower proportion and/or amplitudes of negative readiness potentials and increase occurrence of positive readiness potentials.

8.2. Markers of neuromuscular fatigue

Results in this study are in line with previously reported during fatigue-related decreased torque (Dekerle et al. 2019b) and PVAL (Akagi et al. 2020; Kawakami et al. 2000; Spring et al. 2016), and increased RPE (Keller et al. 2001; Søgaard et al. 2006; Spring et al. 2016; Taylor & Gandevia 2006). The slower rate of torque decline during last half of the fatigue pro-

tocol might be related to larger contribution from more fatigue-resistant SOL muscle (Kawakami et al. 2000). Change in CVAL was in line with studies using fatiguing isometric knee extensions reporting declines of 8–9% (Dekerle et al. 2019a) and ~13% (Dekerle et al. 2019b) despite higher initial CVAL in these studies. Increased SITs during both CVAL and PVAL is explained by suboptimal drive of α-motoneurons and muscle fibres, and a reserve in cortical and motoneuronal output (Todd et al. 2016). PVAL decreased significantly after Block1 and Block2, whereas CVAL decrease was only significant after Block2. Different VAL dynamics point out that fatigue shifted to more higher levels of the corticospinal pathway as fatigue progressed or that there were changes how stimulus activated spinal motoneuron pools of agonist, antagonist and synergist muscles. High force production levels and early fatigue have been linked to peripheral fatigue (Gandevia 2001), and possible mechanisms include changes in the axons of α-motoneurons, neuromuscular junction, sarcolemmal signal transmission and contractility of the muscle fibres (Kawakami et al. 2000; Sieck & Prakash 1995).

Corticospinal excitability during fatigue in submaximal plantar flexion has been shown to increase (Hoffman et al. 2009; Iguchi & Shields 2012). In contrast, Kirk et al. (2019) showed a reduced MEP during brief MVC after fatiguing submaximal intermittent isometric plantar flexions. Overall MEPs increase or show no change during submaximal and maximal contractions during fatigue (table 1), which is supported by the trend of increased corticospinal excitability during fatigue in this study. Decreased responsiveness of corticospinal motoneurons during fatigue (McNeil et al. 2011) is compensated by cortical mechanisms related to increased and stronger recruitment of corticofugal cells, and a decrease in cortical inhibition of corticospinal motoneurons which are also the mechanisms behind increase in MEP size (Gandevia 2001) and EMG activity (Taylor & Gandevia 2008).

Cortical silent period has been shown to increase during fatigue (Benwell et al. 2007; Iguchi & Shields 2012). One possible mechanism is related to increased III/IV afferent activity (Kennedy et al. 2016; Sidhu et al. 2017). In contrast cortical silent period has been shown to shorten (Kirk et al. 2019) or remain unchanged (Gandevia 2001) during MVCs. Large stimulus intensities have shown to increase cortical silent period and low intensities to shorten (Gandevia 2001). Shortened cortical silent period in this study might be explained by intermittent fatigue and CVAL assessment protocol which enabled reperfusion in the muscles and reduced III/IV afferent activity. Another possibility is high voluntary effort and torque output

level during CVAL contractions, that have previously shown to shorten cortical silent period (Matsugi 2019). While not instructed in this study it has been shown that cortical silent period is shortened if subjects are instructed to try to rebound torque level after stimulus (Mathis et al. 1998) meaning that motivation can increase drive from M1 cortex despite of fatigue.

8.3. Limitations and future directions

Substantial amount of trials due to artefacts related to head and eye movement were rejected which affected readiness potential results. This also affected the readiness potential slope occurrences. Also inter-trial and inter-subject RFD variance and sweat-related changes in EEG electrodes impedance may have affected the readiness potential amplitude. For few subjects electrode contact had to be maintained between contractions, but no visible drying of electrodes was observed. Cortical stimulation measures had challenges related to head movement during MVCs and overall discomfort resulted from long duration sitting. CVAL is known to be affected by antagonist activation and possible non-linearity related to torque–SIT relationship (Todd et al. 2016). During CVAL assessment large EMG drifts were observed, which might have affected the accuracy of cortical silent period analysis. Corticospinal excitability sigmoid fit was partly affected by the narrow stimulus intensity range resulting in unsaturated responses after fatigue protocol.

This study enabled planning of more repeatable measurements of MEP responses during low muscle activity with the help of timer and force trace guidance system and automatically applied stimuli. This automation made it possible to measure CNS function with minimal recovery after fatiguing contractions and perhaps condition subjects CNS during stimulus. CNS is known to recover considerable amount under one minute even when muscle activation is maintained with electric stimulation (Löscher et al. 1996) and discharge rates of motoneurons have shown to recover fully in 3-min (Bigland–Ritchie et al. 1986). Also significant peripheral recovery happens during first minutes after fatiguing exercise (Dekerle et al. 2019a). In future more attention must be paid on subject instructions in self-started force productions to reduce sources of artefacts. Another possibility to counteract high rejection count is to increase number of trials. More fatigue studies with slope-depended readiness potentials and conditioned RFDs are needed to fully understand the relationship between positive and negative readiness potentials and fatigue.

Applicability. Testing protocol was very demanding and discomfortable for the subjects. All participants had athletic background and were familiar with high effort physical work. High intensity TMS stimulation during submaximal contractions above 50%MVC is physically and mentally intense, and might cause feelings of anxiety and fear. Requirement of calmness during severe fatigue and modest pain sensation is challenging. The results of this study are therefore applicable for mentally strong athletic men population. Because of small number of valid trials, several artefact factors and small number of subjects reserve is recommended towards results.

9. CONCLUSION

The goal of this study was to explore connection between unconscious movement preparation and state of corticospinal pathway during fatigue, and if premotor activity (readiness potential) could predict changes in cortical TMS measurements recruitment curve and cortical voluntary activation, respectively. Reversal phase-dependent change in readiness potential slope occurrences was shown between fatigue and control conditions. Corticospinal excitability increased similarly after high and low torque level intermittent plantarflexor contractions. Different temporal modulation of CVAL and PVAL showed that peripheral fatigue was more dominant in the first half of the fatigue protocol and central fatigue in the later half. Negative relationship was found between change in positive readiness potential late component amplitude and decrease in torque during fatigue, which shows individual differences in the initial state of neuronal circuits at M1 cortex and how fatigue is compensated by shifting cortical neural circuits into more favourable state for movement ignition.

REFERENCES

Abbiss, C. R., Peiffer, J. J., Meeusen, R. & Skorski, S. 2015. Role of Ratings of Perceived Exertion during Self-Paced Exercise: What are We Actually Measuring? Sports Medicine 45 (9), 1235–1243.

Akagi, R., Imaizumi, N., Sato, S., Hirata, N., Tanimoto, H. & Hirata, K. 2020. Active recovery has a positive and acute effect on recovery from fatigue induced by repeated maximal voluntary contractions of the plantar flexors. Journal of Electromyography and Kinesiology 50 (December 2019), 102384.

Ali, A., Moss, C., Yoo, M. J. Y., Wilkinson, A. & Breier, B. H. 2017. Effect of mouth rinsing and ingestion of carbohydrate solutions on mood and perceptual responses during exercise. Journal of the International Society of Sports Nutrition 14 (1), 4.

Andersen, B., Westlund, B. & Krarup, C. 2003. Failure of activation of spinal motoneurones after muscle fatigue in healthy subjects studied by transcranial magnetic stimulation. Journal of Physiology 551 (1), 345–356.

Arai, N., Lu, M. K., Ugawa, Y. & Ziemann, U. 2012. Effective connectivity between human supplementary motor area and primary motor cortex: A paired-coil TMS study. Experimental Brain Research 220 (1), 79–87.

Arendt–Nielsen, L., Mills, K. R. & Forster, A. 1989. Changes in muscle fiber conduction velocity, mean power frequency, and mean EMG voltage during prolonged submaximal contractions. Muscle & Nerve 12 (6), 493–497.

Atasavun Uysal, S. & Düger, T. 2020. Motor control and sensory-motor integration of human movement. In Comparative Kinesiology of the Human Body (pp. 443–452). Elsevier.

Bailey, S. P., Davis, J. M. & Ahlborn, E. N. 1993. Neuroendocrine and substrate responses to altered brain 5-HT activity during prolonged exercise to fatigue. Journal of Applied Physiology 74 (6), 3006–3012.

Bäumer, T., Schippling, S., Kroeger, J., Zittel, S., Koch, G., Thomalla, G., Rothwell, J. C., Siebner, H. R., Orth, M. & Münchau, A. 2009. Inhibitory and facilitatory connectivity from ventral premotor to primary motor cortex in healthy humans at rest - A bifocal TMS study. Clinical Neurophysiology 120 (9), 1724–1731.

Benwell, N. M., Mastaglia, F. L. & Thickbroom, G. W. 2007. Differential changes in long-interval intracortical inhibition and silent period duration during fatiguing hand exercise. Experimental Brain Research 179 (2), 255–262.

Berchicci, M., Menotti, F., Macaluso, A. & Di Russo, F. 2013. The neurophysiology of central and peripheral fatigue during sub-maximal lower limb isometric contractions. Frontiers in Human Neuroscience 7 (MAR).

Berridge, C. W. & Waterhouse, B. D. 2003. The locus coeruleus-noradrenergic system: Modulation of behavioral state and state-dependent cognitive processes. Brain Research Reviews 42 (1), 33–84.

Bigland–Ritchie, B. R., Dawson, N. J., Johansson, R. S. & Lippold, O. C. 1986. Reflex origin for the slowing of motoneurone firing rates in fatigue of human voluntary contractions. The Journal of Physiology 379 (1), 451–459.

Bigland−Ritchie, B. & Woods, J. J. 1984. Changes in muscle contractile properties and neural control during human muscular fatigue. Muscle & Nerve 7 (9), 691–699.

Blackwood, D. H. R. & Muir, W. J. 1990. Cognitive brain potentials and their application. British Journal of Psychiatry 157 (DEC. SUPPL. 9), 96–101.

Bongiovanni, L. G. & Hagbarth, K. E. 1990. Tonic vibration reflexes elicited during fatigue from maximal voluntary contractions in man. The Journal of Physiology 423 (1), 1–14.

Bowtell, J. L., Mohr, M., Fulford, J., Jackman, S. R., Ermidis, G., Krustrup, P. & Mileva, K. N. 2018. Improved Exercise Tolerance with Caffeine Is Associated with Modulation of both Peripheral and Central Neural Processes in Human Participants. Frontiers in Nutrition 5.

Butler, J. E., Taylor, J. L. & Gandevia, S. C. 2003. Responses of Human Motoneurons to Corticospinal Stimulation during Maximal Voluntary Contractions and Ischemia. Journal of Neuroscience 23 (32), 10224–10230.

Carson, R. G., Nelson, B. D., Buick, A. R., Carroll, T. J., Kennedy, N. C. & Cann, R. Mac. 2013. Characterizing changes in the excitability of corticospinal projections to proximal muscles of the upper limb. Brain Stimulation 6 (5), 760–768.

Chen, R., Yaseen, Z., Cohen, L. G. & Hallett, M. 1998. Time course of corticospinal excitability in reaction time and self- paced movements. Annals of Neurology 44 (3), 317–325.

Chouinard, P. A. & Paus, T. 2006. The Primary Motor and Premotor Areas of the Human Cerebral Cortex. The Neuroscientist 12 (2), 143–152.

Cisek, P. & Kalaska, J. F. 2010. Neural mechanisms for interacting with a world full of action choices. Annual Review of Neuroscience 33 (1), 269–298.

Cordeiro, L. M. S., Rabelo, P. C. R., Moraes, M. M., Teixeira-Coelho, F., Coimbra, C. C., Wanner, S. P. & Soares, D. D. 2017. Physical exercise-induced fatigue: The role of serotonergic and dopaminergic systems. Brazilian Journal of Medical and Biological Research 50 (12).

Crewe, H., Tucker, R. & Noakes, T. D. 2008. The rate of increase in rating of perceived exertion predicts the duration of exercise to fatigue at a fixed power output in different environmental conditions. European Journal of Applied Physiology 103 (5), 569–577.

Cui, R. Q. & Deecke, L. 1999. High resolution DC EEG of the Bereitschaftspotential preceding anatomically congruent versus spatially congruent bimanual finger movements. Brain Topography 12 (2), 117–127.

Dalsgaard, M. K., Ide, K., Cai, Y., Quistorff, B. & Secher, N. H. 2002. The intent exercise influences the cerebral O2/carbohydrate uptake ration in humans. Journal of Physiology 540 (2), 681–689.

Davare, M., Andres, M., Cosnard, G., Thonnard, J. L. & Olivier, E. 2006. Dissociating the role of ventral and dorsal premotor cortex in precision grasping. Journal of Neuroscience 26 (8), 2260–2268.

de Morree, H. M., Klein, C. & Marcora, S. M. 2012. Perception of effort reflects central motor command during movement execution. Psychophysiology 49 (9), 1242–1253.

Deecke, L., Grözinger, B. & Kornhuber, H. H. 1976. Voluntary finger movement in man: Cerebral potentials and theory. Biological Cybernetics 23 (2), 99–119.

Dekerle, J., Ansdell, P., Schäfer, L., Greenhouse-Tucknott, A. & Wrightson, J. 2019a. Methodological issues with the assessment of voluntary activation using transcranial magnetic stimulation in the knee extensors. European Journal of Applied Physiology 119 (4), 991–1005.

Dekerle, J., Greenhouse-Tucknott, A., Wrightson, J. G., Schäfer, L. & Ansdell, P. 2019b. Improving the measurement of TMS-assessed voluntary activation in the knee extensors. PLoS ONE 14 (6).

Dienel, G. A. & Rothman, D. L. 2019. Glycogenolysis in Cerebral Cortex During Sensory Stimulation, Acute Hypoglycemia, and Exercise: Impact on Astrocytic Energetics, Aerobic Glycolysis, and Astrocyte-Neuron Interactions. In Advances in Neurobiology (Vol. 23, pp. 209–267).

Duchateau, J., Balestra, C., Carpentier, A. & Hainaut, K. 2002. Reflex regulation during sustained and intermittent submaximal contractions in humans. Journal of Physiology 541 (3), 959–967.

Duque, J., Labruna, L., Verset, S., Olivier, E. & Ivry, R. B. 2012. Dissociating the role of prefrontal and premotor cortices in controlling inhibitory mechanisms during motor preparation. Journal of Neuroscience 32 (3), 806–816.

Emmons, E. B., De Corte, B. J., Kim, Y., Parker, K. L., Matell, M. S. & Narayanan, N. S. 2017. Rodent medial frontal control of temporal processing in the dorsomedial striatum. Journal of Neuroscience 37 (36), 8718–8733.

Enoka, R. M. & Stuart, D. G. 1985. The contribution of neuroscience to exercise studies. Federation Proceedings 44 (7), 2279–2285.

Enoka, R. M. & Duchateau, J. 2016. Translating fatigue to human performance. Medicine and Science in Sports and Exercise 48 (11), 2228–2238.

Farrant, M. & Nusser, Z. 2005. Variations on an inhibitory theme: Phasic and tonic activation of GABA A receptors. Nature Reviews Neuroscience 6 (3), 215–229.

Fifel, K. 2018. Readiness potential and neuronal determinism: New insights on libet experiment. Journal of Neuroscience 38 (4), 784–786.

Finn, H., Rouffet, D. M., Kennedy, D. S., Green, S. & Taylor, J. L. 2018. Motoneuron excitability of the quadriceps decreases during a fatiguing submaximal isometric contraction. Journal of Applied Physiology 124 (4), 970–979.

Fitch, S. & McComas, A. 1985. Influence of human muscle length on fatigue. The Journal of Physiology 362 (1), 205–213.

Foley, T. E. & Fleshner, M. 2008. Neuroplasticity of dopamine circuits after exercise: Implications for central fatigue. NeuroMolecular Medicine 10 (2), 67–80.

Fortney, S. M. & Vroman, N. B. 1985. Exercise, Performance and Temperature Control: Temperature Regulation during Exercise and Implications for Sports Performance and Training. Sports Medicine: An International Journal of Applied Medicine and Science in Sport and Exercise 2 (1), 8–20.

Freude, G. & Ullsperger, P. 1987. Changes in Bereitschaftspotential during fatiguing and non-fatiguing hand movements. European Journal of Applied Physiology and Occupational Physiology 56 (1), 105–108.

Gandevia, S. C. 2001. Spinal and supraspinal factors in human muscle fatigue. Physiological Reviews 81 (4), 1725–1789.

Gandevia, S. C., Petersen, N., Butler, J. E. & Taylor, J. L. 1999. Impaired response of human motoneurones to corticospinal stimulation after voluntary exercise. Journal of Physiology 521 (3), 749–759.

Gant, N., Stinear, C. M. & Byblow, W. D. 2010. Carbohydrate in the mouth immediately facilitates motor output. Brain Research 1350, 151–158.

Garland, S. J. 1991. Role of small diameter afferents in reflex inhibition during human muscle fatigue. The Journal of Physiology 435 (1), 547–558.

Gerdle, B. & Fugl‐Meyer, A. R. 1992. Is the mean power frequency shift of the EMG a selective indicator of fatigue of the fast twitch motor units? Acta Physiologica Scandinavica 145 (2), 129–138.

Gibson, A. S. C., Lambert, E. V., Rauch, L. H. G., Tucker, R., Baden, D. A., Foster, C. & Noakes, T. D. 2006. The role of information processing between the brain and peripheral physiological systems in pacing and perception of effort. Sports Medicine 36 (8), 705–722.

Gramfort, A., Luessi, M., Larson, E., Engemann, D. A., Strohmeier, D., Brodbeck, C., Goj, R., Jas, M., Brooks, T., Parkkonen, L. & Hämäläinen, M. 2013. MEG and EEG data analysis with MNE-Python. Frontiers in Neuroscience 7 (7 DEC).

Gruet, M., Temesi, J., Rupp, T., Levy, P., Millet, G. Y. & Verges, S. 2013. Stimulation of the motor cortex and corticospinal tract to assess human muscle fatigue. Neuroscience 231, 384–399.

Hadoush, H., Tobimatsu, Y., Nagatomi, A., Kimura, H., Ito, Y. & Maejima, H. 2009. Monopolar surface electromyography: A better tool to assess motoneuron excitability upon passive muscle stretching. Journal of Physiological Sciences 59 (3), 243–247.

Haggard, P. & Tsakiris, M. 2009. The experience of agency: Feelings, judgments, and responsibility. Current Directions in Psychological Science 18 (4), 242–246.

Haile, L., Gallagher, M., J. Robertson, R., Haile, L., Gallagher, M. & J. Robertson, R. 2015. Perceived Exertion. In Perceived Exertion Laboratory Manual (pp. 11–20). New York, NY: Springer New York.

Hansen, N. B., Nowicki, P. T., Miller, R. R., Malone, T., Bickers, R. G. & Menke, J. A. 1986. Alterations in cerebral blood flow and oxygen consumption during prolonged hypocarbia. Pediatric Research 20 (2), 147–150.

Heckman, C. J., Johnson, M., Mottram, C. & Schuster, J. 2008. Persistent inward currents in spinal motoneurons and their influence on human motoneuron firing patterns. Neuroscientist 14 (3), 264–275.

Henneman, E., Somjen, G. & Carpenter, D. O. 1965. Functional Significance of cell size in spinal motoneurons. Journal of Neurophysiology 28 (3), 560–580.

Hoffman, B. W., Oya, T., Carroll, T. J. & Cresswell, A. G. 2009. Increases in corticospinal responsiveness during a sustained submaximal plantar flexion. Journal of Applied Physiology 107 (1), 112–120.

Hogan, M. C., Richardson, R. S. & Haseler, L. J. 1999. Human muscle performance and PCr hydrolysis with varied inspired oxygen fractions: A 31P-MRS study. Journal of Applied Physiology 86 (4), 1367–1373.

Houk, J. C., Keifer, J. & Barto, A. G. 1993. Distributed motor commands in the limb premotor network. Trends in Neurosciences 16 (1), 27–33.

Hunter, S. K. 2018. Performance fatigability: Mechanisms and task specificity. Cold Spring Harbor Perspectives in Medicine 8 (7), a029728.

Hureau, T. J., Romer, L. M. & Amann, M. 2018. The 'sensory tolerance limit': A hypothetical construct determining exercise performance? European Journal of Sport Science 18 (1), 13–24.

Ide, K., Schmalbruch, I. K., Quistorff, B., Horn, A. & Secher, N. H. 2000. Lactate, glucose and O2 uptake in human brain during recovery from maximal exercise. Journal of Physiology 522 (1), 159–164.

Iguchi, M. & Shields, R. K. 2012. Cortical and segmental excitability during fatiguing contractions of the soleus muscle in humans. Clinical Neurophysiology 123 (2), 335–343.

Ikeda, A., Lüders, H. O., Shibasaki, H., Collura, T. F., Burgess, R. C., Morris, H. H. & Hamano, T. 1995. Movement-related potentials associated with bilateral simultaneous and unilateral movements recorded from human supplementary motor area. Electroencephalography and Clinical Neurophysiology 95 (5), 323–334.

Jacobs, I. & Bell, D. G. 2004. Effects of acute modafinil ingestion on exercise time to exhaustion. Medicine and Science in Sports and Exercise 36 (6), 1078–1082.

Jankelowitz, S. K. & Colebatch, J. G. 2002. Movement-related potentials associated with self-paced, cued and imagined arm movements. Experimental Brain Research 147 (1), 98–107.

Jas, M., Engemann, D. A., Bekhti, Y., Raimondo, F. & Gramfort, A. 2017. Autoreject: Automated artifact rejection for MEG and EEG data. NeuroImage 159, 417–429.

Jiang, Z., Wang, X. F., Kisiel-Sajewicz, K., Yan, J. H. & Yue, G. H. 2012. Strengthened functional connectivity in the brain during muscle fatigue. NeuroImage 60 (1), 728–737.

Jiang, Z., Wang, X. F. & Yue, G. H. 2016. Strengthened Corticosubcortical Functional Connectivity during Muscle Fatigue. Neural Plasticity 2016, 1–11.

Jo, H. G., Hinterberger, T., Wittmann, M., Borghardt, T. L. & Schmidt, S. 2013. Spontaneous EEG fluctuations determine the readiness potential: Is preconscious brain activation a preparation process to move? Experimental Brain Research 231 (4), 495–500.

Johnston, J., Rearick, M. & Slobounov, S. 2001. Movement-related cortical potentials associated with progressive muscle fatigue in a grasping task. Clinical Neurophysiology 112 (1), 68–77.

Jubeau, M., Rupp, T., Temesi, J., Perrey, S., Wuyam, B., Millet, G. Y. & Verges, S. 2017. Neuromuscular Fatigue during Prolonged Exercise in Hypoxia. Medicine and Science in Sports and Exercise 49 (3), 430–439.

Juel, C. 1988. Muscle action potential propagation velocity changes during activity. Muscle & Nerve 11 (7), 714–719.

Kato, M. & Tanji, J. 1972. Cortical motor potentials accompanying volitionally controlled single motor unit discharges in human finger muscles. Brain Research 47 (1), 103–111.

Kawakami, Y., Amemiya, K., Kanehisa, H., Ikegawa, S. & Fukunaga, T. 2000. Fatigue responses of human triceps surae muscles during repetitive maximal isometric contractions. Journal of Applied Physiology 88 (6), 1969–1975.

Keller, C., Steensberg, A., Pilegaard, H., Osada, T., Saltin, B., Pedersen, B. K. & Neufer, P. D. 2001. Transcriptional activation of the IL-6 gene in human contracting skeletal muscle: influence of muscle glycogen content. The FASEB Journal: Official Publication of the Federation of American Societies for Experimental Biology 15 (14), 2748–2750.

Keller, M. L., Pruse, J., Yoon, T., Schlinder-Delap, B., Harkins, A. & Hunter, S. K. 2011. Supraspinal fatigue is similar in men and women for a low-force fatiguing contraction. Medicine and Science in Sports and Exercise 43 (10), 1873–1883.

Kennedy, D. S., McNeil, C. J., Gandevia, S. C. & Taylor, J. L. 2016. Effects of fatigue on corticospinal excitability of the human knee extensors. Experimental Physiology 101 (12), 1552–1564.

Kirk, B. J. C., Trajano, G. S., Pulverenti, T. S., Rowe, G. & Blazevich, A. J. 2019. Neuromuscular factors contributing to reductions in muscle force after repeated, high-intensity muscular efforts. Frontiers in Physiology 10 (JUN).

Kirsch, R. F. & Rymer, W. Z. 1987. Neural compensation for muscular fatigue: Evidence for significant force regulation in man. Journal of Neurophysiology 57 (6), 1893–1910.

Klass, M., Lévénez, M., Enoka, R. M. & Duchateau, J. 2008. Spinal mechanisms contribute to differences in the time to failure of submaximal fatiguing contractions performed with different loads. Journal of Neurophysiology 99 (3), 1096–1104.

Klass, M., Roelands, B., LIvInez, M., Fontenelle, V., Pattyn, N., Meeusen, R. & Duchateau, J. 2012. Effects of noradrenaline and dopamine on supraspinal fatigue in well-trained men. Medicine and Science in Sports and Exercise 44 (12), 2299–2308.

Koepp, M. J., Gunn, R. N., Lawrence, A. D., Cunningham, V. J., Dagher, A., Jones, T., Brooks, O. J., Bench, C. J. & Grasby, P. M. 1998. Evidence for striatal dopamine release during a video game. Nature 393 (6682), 266–268.

Kukke, S. N., Paine, R. W., Chao, C. C., De Campos, A. C. & Hallett, M. 2014. Efficient and reliable characterization of the corticospinal system using transcranial magnetic stimulation. Journal of Clinical Neurophysiology 31 (3), 246–252.

Lännergren, J. & Westerblad, H. 1991. Force decline due to fatigue and intracellular acidification in isolated fibres from mouse skeletal muscle. The Journal of Physiology 434 (1), 307–322.

Latini, S. & Pedata, F. 2001. Adenosine in the central nervous system: Release mechanisms and extracellular concentrations. Journal of Neurochemistry 79 (3), 463–484.

Lattari, E., de Oliveira, B. S., Oliveira, B. R. R., de Mello Pedreiro, R. C., Machado, S. & Neto, G. A. M. 2018. Effects of transcranial direct current stimulation on time limit and ratings of perceived exertion in physically active women. Neuroscience Letters 662, 12–16.

Lee, R. H. & Heckman, C. J. 1999. Enhancement of bistability in spinal motoneurons in vivo by the noradrenergic α1 agonist methoxamine. Journal of Neurophysiology 81 (5), 2164–2174.

Liu, J. Z., Yao, B., Siemionow, V., Sahgal, V., Wang, X., Sun, J. & Yue, G. H. 2005. Fatigue induces greater brain signal reduction during sustained than preparation phase of maximal voluntary contraction. Brain Research 1057 (1–2), 113–126.

Löscher, W. N., Cresswell, A. G. & Thorstensson, A. 1996. Central fatigue during a long-lasting submaximal contraction of the triceps surae. Experimental Brain Research 108 (2), 305–314.

Martin, P. G., Smith, J. L., Butler, J. E., Gandevia, S. C. & Taylor, J. L. 2006. Fatigue-sensitive afferents inhibit extensor but not flexor motoneurons in humans. Journal of Neuroscience 26 (18), 4796–4802.

Mathis, J., De Quervain, D. & Hess, C. W. 1998. Dependence of the transcranially induced silent period on the "instruction set" and the individual reaction time. Electroencephalography and Clinical Neurophysiology - Electromyography and Motor Control 109 (5), 426–435.

Matsugi, A. 2019. Changes in the cortical silent period during force control. Somatosensory & Motor Research 36 (1), 8–13.

Matsui, T., Omuro, H., Liu, Y. F., Soya, M., Shima, T., Mcewen, B. S. & Soya, H. 2017. Astrocytic glycogen-derived lactate fuels the brain during exhaustive exercise to maintain endurance capacity. Proceedings of the National Academy of Sciences of the United States of America 114 (24), 6358–6363.

Matsui, T., Soya, M. & Soya, H. 2019. Endurance and Brain Glycogen: A Clue Toward Understanding Central Fatigue. In Advances in Neurobiology (Vol. 23, pp. 331–346).

Matsui, T., Soya, S., Okamoto, M., Ichitani, Y., Kawanaka, K. & Soya, H. 2011. Brain glycogen decreases during prolonged exercise. The Journal of Physiology 589 (13), 3383–3393.

McCormick, A., Meijen, C. & Marcora, S. 2015. Psychological Determinants of Whole-Body Endurance Performance. Sports Medicine 45 (7), 997–1015.

McDonnell, M. N., Orekhov, Y. & Ziemann, U. 2006. The role of GABAB receptors in intracortical inhibition in the human motor cortex. Experimental Brain Research 173 (1), 86–93.

McMorris, T., Barwood, M. & Corbett, J. 2018. Central fatigue theory and endurance exercise: Toward an interoceptive model. Neuroscience and Biobehavioral Reviews 93, 93–107.

McNeil, C. J., Giesebrecht, S., Gandevia, S. C. & Taylor, J. L. 2011. Behaviour of the motoneurone pool in a fatiguing submaximal contraction. Journal of Physiology 589 (14), 3533–3544.

McNeil, C. J., Martin, P. G., Gandevia, S. C. & Taylor, J. L. 2009. The response to paired motor cortical stimuli is abolished at a spinal level during human muscle fatigue. Journal of Physiology 587 (23), 5601–5612.

Meeusen, R., Roeykens, J., Magnus, L., Keizer, H. & De Meirleir, K. 1997. Endurance performance in humans: The effect of a dopamine precursor or a specific serotonin (5-HT(2A/2C)) antagonist. International Journal of Sports Medicine 18 (8), 571–577.

Meeusen, R., Watson, P. & Dvorak, J. 2006. The brain and fatigue: New opportunities for nutritional interventions? Journal of Sports Sciences 24 (7), 773–782.

Mense, S. 1983. Basic neurobiologic mechanisms of pain and analgesia. The American Journal of Medicine 75 (5 PART 1), 4–14.

MNE-Python ICA API. 2020.

Morales–Alamo, D., Losa–Reyna, J., Torres–Peralta, R., Martin–Rincon, M., Perez–Valera, M., Curtelin, D., Ponce–González, J. G., Santana, A. & Calbet, J. A. L. 2015. What limits performance during whole-body incremental exercise to exhaustion in humans? Journal of Physiology 593 (20), 4631–4648.

Münchau, A., Bloem, B. R., Irlbacher, K., Trimble, M. R. & Rothwell, J. C. 2002. Functional connectivity of human premotor and motor cortex explored with repetitive transcranial magnetic stimulation. Journal of Neuroscience 22 (2), 554–561.

Murakami, K., Fujisawa, H., Onobe, J. & Sato, Y. 2014. Relationship between muscle fiber conduction velocity and the force-time curve during muscle twitches. Journal of Physical Therapy Science 26 (4), 621–624.

Myers, S. & Pugsley, T. A. 1986. Decrease in rat straital dopamine synthesis and metabolism in vivo by metabolically stable adenosine receptor agonists. Brain Research 375 (1), 193–197.

Nachev, P., Kennard, C. & Husain, M. 2008. Functional role of the supplementary and pre-supplementary motor areas. Nature Reviews Neuroscience 9 (11), 856–869.

Nielsen, B., Hyldig, T., Bidstrup, F., González-Alonso, J. & Christoffersen, G. R. J. 2001. Brain activity and fatigue during prolonged exercise in the heat. Pflugers Archiv European Journal of Physiology 442 (1), 41–48.

Noakes, T. D., St. Clair Gibson, A. & Lambert, E. V. 2005. From catastrophe to complexity: A novel model of integrative central neural regulation of effort and fatigue during exercise in humans: Summary and conclusions. British Journal of Sports Medicine 39 (2), 120–124.

Nybo, L., Møller, K., Pedersen, B. K., Nielsen, B. & Secher, N. H. 2003. Association between fatigue and failure to preserve cerebral energy turnover during prolonged exercise. Acta Physiologica Scandinavica 179 (1), 67–74.

Nybo, L. 2003. CNS fatigue and prolonged exercise: Effect of glucose supplementation. Medicine and Science in Sports and Exercise 35 (4), 589–594.

Nybo, L., Møller, K., Volianitis, S., Nielsen, B. & Secher, N. H. 2002. Effects of hyperthermia on cerebral blood flow and metabolism during prolonged exercise in humans. Journal of Applied Physiology 93 (1), 58–64.

Nybo, L. & Nielsen, B. 2001a. Perceived exertion is associated with an altered brain activity during exercise with progressive hyperthermia. Journal of Applied Physiology 91 (5), 2017–2023.

Nybo, L. & Nielsen, B. 2001b. Middle cerebral artery blood velocity is reduced with hyperthermia during prolonged exercise in humans. Journal of Physiology 534 (1), 279–286.

Nybo, L., Rasmussen, P. & Sawka, M. N. 2014. Performance in the heat-physiological factors of importance for hyperthermia-induced fatigue. Comprehensive Physiology 4 (2), 657–689.

Nybo, L. & Secher, N. H. 2004. Cerebral perturbations provoked by prolonged exercise. Progress in Neurobiology 72 (4), 223–261.

Paradiso, G., Saint-Cyr, J. A., Lozano, A. M., Lang, A. E. & Chen, R. 2003. Involvement of the human subthalamic nucleus in movement preparation. Neurology 61 (11), 1538–1545.

Paradiso, G., Cunic, D., Saint-Cyr, J. A., Hoque, T., Lozano, A. M., Lang, A. E. & Chen, R. 2004. Involvement of human thalamus in the preparation of self-paced movement. Brain 127 (12), 2717–2731.

Pedersen, T. H., De Paoli, F. & Nielsen, O. B. 2005. Increased excitability of acidified skeletal muscle: Role of chloride conductance. Journal of General Physiology 125 (2), 237–246.

Périard, J. D., De Pauw, K., Zanow, F. & Racinais, S. 2018. Cerebrocortical activity during self-paced exercise in temperate, hot and hypoxic conditions. Acta Physiologica 222 (1), e12916.

Perry, B. G., Cotter, J. D., Mejuto, G., Mündel, T. & Lucas, S. J. E. 2014. Cerebral hemodynamics during graded valsalva maneuvers. Frontiers in Physiology 5.

Petersen, N. T., Taylor, J. L., Butler, J. E. & Gandevia, S. C. 2003. Depression of activity in the corticospinal pathway during human motor behavior after strong voluntary contractions. Journal of Neuroscience 23 (22), 7974–7980.

Piitulainen, H., Holobar, A. & Avela, J. 2012. Changes in motor unit characteristics after eccentric elbow flexor exercise. Scandinavian Journal of Medicine and Science in Sports 22 (3), 418–429.

Piitulainen, H. 2010. Functional Adaptation of Sarcolemma to Physical Stress. University of Jyväskylä. Studies in sport, physical education and health 150.

Piitulainen, H., Komi, P., Linnamo, V. & Avela, J. 2008. Sarcolemmal excitability as investigated with M-waves after eccentric exercise in humans. Journal of Electromyography and Kinesiology 18 (4), 672–681.

Plewnia, C., Hoppe, J., Hiemke, C., Bartels, M., Cohen, L. G. & Gerloff, C. 2002. Enhancement of human cortico-motoneuronal excitability by the selective norepinephrine reuptake inhibitor reboxetine. Neuroscience Letters 330 (3), 231–234.

Purves, D., Augustine, G. J., Fitzpatrick, D., Hall, W. C., LaMantia, A.-S., Mooney, R. D., Platt, M. L. & White, L. E. (Eds.). 2018. Neuroscience (6th ed.). New York, NY: Oxford University Press.

Rejeski, W. J. & Ribisl, P. M. 2016. Expected Task Duration and Perceived Effort: An Attributional Analysis. Journal of Sport Psychology 2 (3), 227–236.

Rektor, I., Bareš, M. & Kubová, D. 2001. Movement-related potentials in the basal ganglia: A SEEG readiness potential study. Clinical Neurophysiology 112 (11), 2146–2153.

Robertson, C. V. & Marino, F. E. 2015. Prefrontal and motor cortex EEG responses and their relationship to ventilatory thresholds during exhaustive incremental exercise. European Journal of Applied Physiology 115 (9), 1939–1948.

Robertson, R. J. & Noble, B. J. 1997. 15 Perception of Physical Exertion. Exercise and Sport Sciences Reviews 25 (1), 407–452.

Robol, E., Fiaschi, A. & Manganotti, P. 2004. Effects of citalopram on the excitability of the human motor cortex: A paired magnetic stimulation study. Journal of the Neurological Sciences 221 (1–2), 41–46.

Roelands, B. & Meeusen, R. 2010. Alterations in central fatigue by pharmacological manipulations of neurotransmitters in normal and high ambient temperature. Sports Medicine 40 (3), 229–246.

Rosenbaum, D. A. 2010. Physiological Foundations. In Human Motor Control (pp. 43–91). Elsevier.

Rossman, M. J., Venturelli, M., Mcdaniel, J., Amann, M. & Richardson, R. S. 2012. Muscle mass and peripheral fatigue: A potential role for afferent feedback? Acta Physiologica 206 (4), 242–250.

Rozand, V., Grosprêtre, S., Stapley, P. J. & Lepers, R. 2015. Assessment of neuromuscular function using percutaneous electrical nerve stimulation. Journal of Visualized Experiments 2015 (103).

Ruotsalainen, I., Ahtiainen, J. P., Kidgell, D. J. & Avela, J. 2014. Changes in corticospinal excitability during an acute bout of resistance exercise in the elbow flexors. European Journal of Applied Physiology 114 (7), 1545–1553.

Samii, A., Wassermann, E. M. & Hallett, M. 1997. Decreased postexercise facilitation of motor evoked potentials in patients with cerebellar degeneration. Neurology 49 (2), 538–542.

Sanger, T. D. 2003. Neural population codes. Current Opinion in Neurobiology 13 (2), 238–249.

Schmahmann, J. D. & Pandya, D. N. 1990. Anatomical investigation of projections from thalamus to posterior parietal cortex in the rhesus monkey: A WGA−HRP and fluorescent tracer study. Journal of Comparative Neurology 295 (2), 299–326.

Schubotz, R. I. & Von Cramon, D. Y. 2003. Functional-anatomical concepts of human premotor cortex: Evidence from fMRI and PET studies. NeuroImage 20 (SUPPL. 1), S120–S131.

Schurger, A., Sitt, J. D. & Dehaene, S. 2012. An accumulator model for spontaneous neural activity prior to self-initiated movement. Proceedings of the National Academy of Sciences of the United States of America 109 (42), E2904–E2913.

Shibasaki, H. & Hallett, M. 2006. What is the Bereitschaftspotential? Clinical Neurophysiology 117 (11), 2341–2356.

Shibata, M., Oda, S. & Moritani, T. 1997. The relationships between movement-related cortical potentials and motor unit activity during muscle contraction. Journal of Electromyography and Kinesiology 7 (2), 79–85.

Sidhu, S. K., Weavil, J. C., Mangum, T. S., Jessop, J. E., Richardson, R. S., Morgan, D. E. & Amann, M. 2017. Group III/IV locomotor muscle afferents alter motor cortical and corticospinal excitability and promote central fatigue during cycling exercise. Clinical Neurophysiology 128 (1), 44–55.

Sidhu, S. K., Weavil, J. C., Thurston, T. S., Rosenberger, D., Jessop, J. E., Wang, E., Richardson, R. S., McNeil, C. J. & Amann, M. 2018. Fatigue-related group III/IV muscle afferent feedback facilitates intracortical inhibition during locomotor exercise. Journal of Physiology 596 (19), 4789–4801.

Sieck, G. C. & Prakash, Y. S. 1995. Fatigue at the neuromuscular junction: Branch point vs. presynaptic vs. postsynaptic mechanisms. In Advances in Experimental Medicine and Biology (Vol. 384, pp. 83–100).

Škarabot, J., Mesquita, R. N. O., Brownstein, C. G. & Ansdell, P. 2019. Myths and Methodologies: How loud is the story told by the transcranial magnetic stimulation-evoked silent period? Experimental Physiology 104 (5), 635–642.

Slobounov, S., Hallett, M. & Newell, K. M. 2004. Perceived effort in force production as reflected in motor-related cortical potentials. Clinical Neurophysiology 115 (10), 2391–2402.

Smith, J. L., Martin, P. G., Gandevia, S. C. & Taylor, J. L. 2007. Sustained contraction at very low forces produces prominent supraspinal fatigue in human elbow flexor muscles. Journal of Applied Physiology 103 (2), 560–568.

Soares, D. D., Lima, N. R. V., Coimbra, C. C. & Marubayashi, U. 2004. Intracerebroventricular tryptophan increases heating and heat storage rate in exercising rats. Pharmacology Biochemistry and Behavior 78 (2), 255–261.

Søgaard, K., Gandevia, S. C., Todd, G., Petersen, N. T. & Taylor, J. L. 2006. The effect of sustained low-intensity contractions on supraspinal fatigue in human elbow flexor muscles. Journal of Physiology 573 (2), 511–523.

Spielmann, J. M., Laouris, Y., Nordstrom, M. A., Robinson, G. A., Reinking, R. M. & Stuart, D. G. 1993. Adaptation of cat motoneurons to sustained and intermittent extracellular activation. The Journal of Physiology 464 (1), 75–120.

Spring, J. N., Place, N., Borrani, F., Kayser, B. & Barral, J. 2016. Movement-related cortical potential amplitude reduction after cycling exercise relates to the extent of neuromuscular fatigue. Frontiers in Human Neuroscience 10.

Spruston, N. 2008. Pyramidal neurons: Dendritic structure and synaptic integration. Nature Reviews Neuroscience 9 (3), 206–221.

Swart, J., Robert Lindsay, T., Ian Lambert, M., Craig Brown, J. & David Noakes, T. 2012. Perceptual cues in the regulation of exercise performance-physical sensations of exercise and awareness of effort interact as separate cues. British Journal of Sports Medicine 46 (1), 42–48.

Szubski, C., Burtscher, M. & Löscher, W. N. 2007. Neuromuscular fatigue during sustained contractions performed in short-term hypoxia. Medicine and Science in Sports and Exercise 39 (6), 948–954.

Taube, W., Leukel, C., Nielsen, J. B. & Lundbye-Jensen, J. 2015. Repetitive activation of the corticospinal pathway by means of rTMS may reduce the efficiency of corticomotoneuronal synapses. Cerebral Cortex 25 (6), 1629–1637.

Taylor, J. L., Butler, J. E. & Gandevia, S. C. 1999. Altered responses of human elbow flexors to peripheral-nerve and cortical stimulation during a sustained maximal voluntary contraction. Experimental Brain Research 127 (1), 108–115.

Taylor, J. L. & Gandevia, S. C. 2008. A comparison of central aspects of fatigue in submaximal and maximal voluntary contractions. Journal of Applied Physiology 104 (2), 542–550.

Taylor, J. L., Todd, G. & Gandevia, S. C. 2006. Evidence for a supraspinal contribution to human muscle fatigue. Clinical and Experimental Pharmacology and Physiology 33 (4), 400–405.

Temesi, J., Gruet, M., Rupp, T., Verges, S. & Millet, G. Y. 2014. Resting and active motor thresholds versus stimulus-response curves to determine transcranial magnetic stimulation intensity in quadriceps femoris. Journal of NeuroEngineering and Rehabilitation 11 (1), 40.

Todd, G., Butler, J. E., Taylor, J. L. & Gandevia, S. C. 2005. Hyperthermia: A failure of the motor cortex and the muscle. Journal of Physiology 563 (2), 621–631.

Todd, G., Taylor, J. L. & Gandevia, S. C. 2003. Measurement of voluntary activation of fresh and fatigued human muscles using transcranial magnetic stimulation. Journal of Physiology 551 (2), 661–671.

Todd, G., Taylor, J. L. & Gandevia, S. C. 2016. Measurement of voluntary activation based on transcranial magnetic stimulation over the motor cortex. Journal of Applied Physiology 121 (3), 678–686.

Travers, E., Khalighinejad, N., Schurger, A. & Haggard, P. 2020. Do readiness potentials happen all the time? NeuroImage 206, 116286.

Vafaee, M. S., Vang, K., Bergersen, L. H. & Gjedde, A. 2012. Oxygen consumption and blood flow coupling in human motor cortex during intense finger tapping: Implication for a role of lactate. Journal of Cerebral Blood Flow and Metabolism 32 (10), 1859–1868.

Vagg, R., Mogyoros, I., Kiernan, M. C. & Burke, D. 1998. Activity-dependent hyperpolarization of human motor axons produced by natural activity. Journal of Physiology 507 (3), 919–925.

Virtanen, P., Gommers, R., Oliphant, T. E., Haberland, M., Reddy, T., Cournapeau, D., Burovski, E., Peterson, P., Weckesser, W., Bright, J., van der Walt, S. J., Brett, M., Wilson, J., Millman, K. J., Mayorov, N., Nelson, A. R. J., Jones, E., Kern, R., Larson, E., Carey, C. J., Polat, İ., Feng, Y., Moore, E. W., VanderPlas, J., Laxalde, D., Perktold, J., Cimrman, R., Henriksen, I., Quintero, E. A., Harris, C. R., Archibald, A. M., Ribeiro, A. H., Pedregosa, F., van Mulbregt, P., Vijaykumar, A., Bardelli, A. Pietro, Rothberg, A., Hilboll, A., Kloeckner, A., Scopatz, A., Lee, A., Rokem, A., Woods, C. N., Fulton, C., Masson, C., Häggström, C., Fitzgerald, C., Nicholson, D. A., Hagen, D. R., Pasechnik, D. V., Olivetti, E., Martin, E., Wieser, E., Silva, F., Lenders, F., Wilhelm, F., Young, G., Price, G. A., Ingold, G. L., Allen, G. E., Lee, G. R., Audren, H., Probst, I., Dietrich, J. P., Silterra, J., Webber, J. T., Slavič, J., Nothman, J., Buchner, J., Kulick, J., Schönberger, J. L., de Miranda Cardoso, J. V., Reimer, J., Harrington, J., Rodríguez, J. L. C., Nunez-Iglesias, J., Kuczynski, J., Tritz, K., Thoma, M., Newville, M., Kümmerer, M., Bolingbroke, M., Tartre, M., Pak, M., Smith, N. J., Nowaczyk, N., Shebanov, N., Pavlyk, O., Brodtkorb, P. A., Lee, P., McGibbon, R. T., Feldbauer, R., Lewis, S., Tygier, S., Sievert, S., Vigna, S., Peterson, S., More, S., Pudlik, T., Oshima, T., Pingel, T. J., Robitaille, T. P., Spura, T., Jones, T. R., Cera, T., Leslie, T., Zito, T., Krauss, T., Upadhyay, U., Halchenko, Y. O. & Vázquez-Baeza, Y. 2020. Author Correction: SciPy 1.0: fundamental algorithms for scientific computing in Python (Nature Methods, (2020), 17, 3, (261-272)). Nature Methods 17 (3), 352.

Wang, G. J., Volkow, N. D., Fowler, J. S., Franceschi, D., Logan, J., Pappas, N. R., Wong, C. T. & Netusil, N. 2000. PET studies of the effects of aerobic exercise on human striatal dopamine release. Journal of Nuclear Medicine 41 (8), 1352–1356.

Weavil, J. C. & Amann, M. 2018. Corticospinal excitability during fatiguing whole body exercise. In Progress in Brain Research (Vol. 240, pp. 219–246).

Wen, W., Minohara, R., Hamasaki, S., Maeda, T., An, Q., Tamura, Y., Yamakawa, H., Yamashita, A. & Asama, H. 2018. The Readiness Potential Reflects the Reliability of Action Consequence. Scientific Reports 8 (1), 11865.

Wheaton, L. A., Shibasaki, H. & Hallett, M. 2005. Temporal activation pattern of parietal and premotor areas related to praxis movements. Clinical Neurophysiology 116 (5), 1201–1212.

Wilson, J. R., McCully, K. K., Mancini, D. M., Boden, B. & Chance, B. 1988. Relationship of muscular fatigue to pH and diprotonated P(i) in humans: A 31P-NMR study. Journal of Applied Physiology 64 (6), 2333–2339.

Yablonskiy, D. A., Ackerman, J. J. H. & Raichle, M. E. 2000. Coupling between changes in human brain temperature and oxidative metabolism during prolonged visual stimulation. Proceedings of the National Academy of Sciences of the United States of America 97 (13), 7603–7608.

Yamaguchi, K., Kasai, N., Hayashi, N., Yatsutani, H., Girard, O. & Goto, K. 2020. Acute performance and physiological responses to repeated-sprint exercise in a combined hot and hypoxic environment. Physiological Reports 8 (12).

Zagrean, L. 2014. Principles of Neural Science. (E. R. Kandel, J. H. Schwartz, T. M. Jessell, S. A. Siegelbaum, & A. J. Hudspeth, Eds.), Acta Endocrinologica (Bucharest) (5th ed, Vol. 10). New York: McGraw Hill.

Zhang, L. Q. & Zev Rymer, W. 2001. Reflex and intrinsic changes induced by fatigue of human elbow extensor muscles. Journal of Neurophysiology 86 (3), 1086–1094.

Zhao, J., Lai, L., Cheung, S. S., Cui, S., An, N., Feng, W. & Lorenzo, S. 2015. Hot environments decrease exercise capacity and elevate multiple neurotransmitters. Life Sciences 141, 74–80.